

# INFERENCE ABOUT COMPLEX RELATIONSHIPS USING PEAK HEIGHT DATA FROM DNA MIXTURES

Peter J. Green\*  
University of Bristol.

Julia Mortera†  
Università Roma Tre.

May 28, 2022

## Abstract

In both criminal cases and civil cases there is an increasing demand for the analysis of DNA mixtures involving relationships. The goal might be, for example, to identify the contributors to a DNA mixture where the donors may be related, or to infer the relationship between individuals based on a mixture.

This paper introduces an approach to modelling and computation for DNA mixtures involving contributors with arbitrarily complex relationships. It builds on an extension of Jacquard's condensed coefficients of identity, to specify and compute with joint relationships, not only pairwise ones, including the possibility of inbreeding.

The methodology developed is applied to two casework examples involving a missing person, and simulation studies of performance, in which the ability of the methodology to recover complex relationship information from synthetic data with known 'true' family structure is examined.

The methods used to analyse the examples are implemented in the new **KinMix R** package, that extends the **DNAmixtures** package to allow for modelling DNA mixtures with related contributors. **KinMix** inherits from **DNAmixtures** the capacity to deal with mixtures with many contributors, in a time- and space-efficient way.

*Some key words:* Bayesian networks, coefficients of identity, criminal identification, disputed paternity, DNA mixtures, identity by descent, inbreeding, kinship, uncertainty in allele frequencies.

## 1 Introduction

This article is concerned with probabilistic genotyping methods for DNA mixtures based on unlinked autosomal short tandem repeat (STR) markers, under hypotheses about biological relationships involving contributors to the mixture.

STR markers are the mainstay of DNA profiling systems used in forensic science laboratories world-wide. To create the data used in modelling and analysis, the DNA in a biological specimen is extracted, and through a process of polymerase chain reaction (PCR) amplified to create an electropherogram (EPG), a continuous trace that is digitised for analysis. Identifiable segments of this trace correspond to different known loci, called markers, on the genome. The markers used

---

\*School of Mathematics, University of Bristol, Bristol BS8 1TW, UK.

Email: [P.J.Green@bristol.ac.uk](mailto:P.J.Green@bristol.ac.uk)

†Università Roma Tre, Italy.

Email: [julia.mortera@uniroma3.it](mailto:julia.mortera@uniroma3.it)

are chosen to lie far apart in the genome, usually on different chromosomes, so are unlinked, that is statistically independent. Each segment consists of peaks aligned to a known grid, one peak for each possible allele, or genetic variant, at that locus; for STR markers, these alleles take (generally, integer) values giving the repeat count of a short sequence in the genome. The heights of the peaks measure the abundance of that allele at that locus, and collectively carry a great deal of information about the genetic make-up of the original specimen, but are subject to degradation consisting of both random noise and artefacts introduced in the PCR process, for which a statistical model must be constructed.

The usual methodology uses only autosomal loci, that is, markers on the chromosomes that are not sex-linked, and so involve a contribution from each parent. The individual contributions we call genes, and the unordered pair of contributions the genotype. We call the collection of genotypes across all markers the genotype profile of the individual; note that in a statistical language, we regard genes and genotypes as random variables, while alleles are the possible values of a gene.

When a biological specimen is taken from one individual, and handled and processed under ideal conditions, an EPG represents a noisy version of the genotype profile of that one individual; in this case we can talk about genotyping or ‘typing’. In other situations, either through the circumstances in which the sample is obtained (for example, in rape, or other violent assault) or through contamination, the DNA quantified by the EPG comes from two or more individuals; this is a DNA mixture. In both criminal and civil cases, even for simple tasks such as criminal identification or paternity testing, we need methodology for assessing hypotheses about the genetic origin of the DNA based on mixture data. The focus of this paper is to derive and demonstrate principled and practical methods for such tasks, in cases where there are biological relationships involving the contributors. We concentrate on so-called continuous methods using peak height information, as opposed to binary or semi-continuous methods.

More details of the genetic background to the use of STR markers and DNA mixtures can be found in Section 1 of Cowell *et al.* (2015), and also in the recent review article by Mortera (2020). Both the statistical model we use for EPG peak heights, and exact computationally-efficient methods for inference about the genotype profiles of contributors, can be found in Cowell *et al.* (2015). The present article extends the principles and practice of this work to allow for relationships among the contributors and/or to make inferences about such relationships.

It is convenient and natural when modelling peak height data probabilistically to use a hierarchical formulation, with two main layers: the genotype profiles  $\mathbf{n}$  of the contributors, and the peak heights  $\mathbf{z}$  recorded in the electropherogram; the models typically then consist of two components:

- (a)  $p(\mathbf{n})$  – the joint distribution for  $\mathbf{n}$  – parameterised by population allele frequencies, hypotheses about the contributors, etc., and
- (b)  $p(\mathbf{z}|\mathbf{n})$  – the conditional distribution for  $\mathbf{z}$  given  $\mathbf{n}$  – with parameters identifying the peak height model and the proportions of DNA from each of the contributors contained in the mixture.

Inference based on DNA mixtures usually focusses on the comparison between two hypotheses  $\mathcal{H}_p$  and  $\mathcal{H}_0$  concerning the constitution of the mixture, quantified by the likelihood ratio LR for  $\mathcal{H}_p$  versus  $\mathcal{H}_0$ . In this article, these hypotheses will be about (arbitrarily complex) relationships between mixture contributors, and between contributors and other typed individuals. Simple examples of relationship tests we can construct are

- a paternity test given a child’s genotype, where  $\mathcal{H}_p$  and  $\mathcal{H}_0$  respectively state that the putative father is a contributor to the mixture, or that no contributor to the mixture is related to the child, and

- a test for whether contributors to a mixture, perhaps found at a crime scene, are related in a particular way ( $\mathcal{H}_p$ ) or not at all ( $\mathcal{H}_0$ ).

Although above and throughout the paper, we use the words ‘test’ and ‘hypothesis’, etc., that are familiar from statistical hypothesis testing, we should make clear that this is not what we are doing. Rather, we are contrasting alternative explanations of the evidence, by means of  $\log_{10}$  LR values. These ‘weights of evidence’ are to be interpreted in the applicable judicial context, where they will be combined with other evidence, not necessarily quantifiable numerically, rather than referred to a null distribution to yield for example p-values. The  $\log_{10}$  LR scale for weights of evidence is standard in forensic statistics (Balding 2005), but in general usage can be traced back to Turing; see Good (1979). The scale is natural and interpretable: for example a  $\log_{10}$  LR of 6 means that the evidence is  $10^6 = 1,000,000$  times more likely under one hypothesis than another.

Throughout we use the probabilistic and computational formulation for DNA mixtures of Cowell *et al.* (2015), and the software implementation of this in the **DNAmixtures** **R** package of Graversen (2013); the model emulates the PCR process described above, and recognises artefacts including stutter, drop-out, drop-in and silent alleles. Our new model extensions are largely aimed at modelling the genotype profile distribution  $p(\mathbf{n})$  to express complex relationships; the methods are implemented in an **R** package **KinMix** (Green 2020a) that supplements **DNAmixtures**. Early ideas in this direction can be found in Green and Mortera (2017). Although implementation is restricted to this model and this computational environment, the ideas are quite general and could be adapted to other probabilistic genotyping systems, and to other peak height models.

The paper is organised as follows. In Section 2, we propose a formulation and notation for expressing quantitatively the simultaneous relationships among an arbitrary set of individuals, specified through their joint pedigree. This notation generalises long-standing coefficients of relationship applicable only to pairs of individuals, and is useful both for specifying relationships precisely and computing with them. The formulation is completely general, its applicability is not confined to STR markers and DNA mixtures, but encodes relationships for any quantitative genetic analysis. In Section 3, we use this encoding to characterise the joint distribution of genotypes in a family, and thereby develop efficient computational inference schemes for DNA mixtures, using Bayesian network (BN) methods. Section 4 is devoted to BN computations for mixtures where there is an ‘ambient’ level of relatedness across the whole population, rather than specific close relationships, or where allele frequencies are not exactly known. In section 5 we discuss the setting of parameters for likelihood calculations in our model, and in section 6 we introduce the **R** package **KinMix** implementing all of the methods in this paper. Section 7 and 8 illustrate the methodology with some simulated scenarios, and several real case studies, including some comparative timings highlighting the fast computation times that are achieved. Finally, we discuss extensions such as allowing for mutation.

## 2 Encoding relationships via IBD pattern distributions

An essential preliminary to modelling and analysis of DNA mixtures with related contributors is a compact and precise representation of joint relationships among a set of arbitrarily related individuals. Developing and illuminating such a representation is the focus of this section, which is of universal applicability, not confined to mixture analysis.

Under our simplified genetic model of unlinked autosomal STR markers, the sole source of relationship between individuals is *identity by descent* (IBD). This is the phenomenon that two genes may be identical because they are copies of the same ancestor gene, rather than being independent draws from the ‘gene pool’, so that the genotypes of two or more related actors will be positively associated.

It is important to distinguish IBD from *identity by state* (IBS), which includes the possibility that independent draws from the gene pool have the same value by chance. For example, consider a mother–daughter pair, and a single STR marker where the mother’s genotype is say  $(a,b)$ , and the child’s is  $(c,d)$ , where in both cases we have ordered the genes in the genotype as (maternal gene, paternal gene). Then by Mendel’s first law,  $c$  is equal to  $a$  or  $b$  with equal probability, while  $d$  is contributed by the father. The gene  $c$  is identical by descent to either  $a$  or  $b$  respectively, but unless the mother’s and father’s genes are all distinct in value, this is not the only way that any of  $(a,b,c,d)$  can be equal in value (identical by state). For example,  $a$  and  $b$  could by chance be equal (i.e. the mother is homozygous), or  $a$  and  $d$  could be equal, or indeed both.

For other relationships than parent–child, and for relationships among more than two individuals, we need a way to encode the implications of Mendel’s first law for the joint distribution of all the individuals’ genotypes; that is the objective of this section.

A pedigree is a graphical or tabular depiction of the identities of all individuals under consideration, mapping to the identities of their parents, and is a useful compact and precise vehicle for specifying joint relationships. In all of the pedigrees we use and display, either both or neither of the parents are included; those with no parents in the pedigree are called founding individuals, or founders, and their genes are founding genes. Given a pedigree, IBD is determined by the meioses generating the genes of each child given those of its parents, and any inbreeding within or between founding individuals: the actual allelic values are not relevant to this. For two individuals, Table 1 of Thompson (2013) lays out all possible patterns; this table is adapted as our Table 1 below. An explanation of the IBD states is given in Section 2.2. Thompson credits this formulation to Nadot and Vaysseix (1973), although they do not use a tabular representation.

Table 1: The IBD states among the four genes of two individuals  $B_1$  and  $B_2$ , adapted from Table 1 of Thompson (2013). The two gametes of individual  $B_1$  are denoted  $a, b$ , and those of  $B_2$  are  $c$  and  $d$ . The IBD state is defined by the labelling developed by Nadot and Vaysseix (1973), and further explained in Section 2.2. The states can be grouped into subsets of genotypically equivalent states, indicated by the horizontal lines; the total probability of the subset is given on the first row of each. For example,  $\Delta_3$  is the combined probability of states  $(1, 1, 1, 2)$  and  $(1, 1, 2, 1)$ .

IBD state				State		$\kappa$
$B_1$	$B_2$	Description	Probability	Partition	Jacquard	
$a$	$b$	$c$	$d$			–
1	1	1	1	$(a, b, c, d)$	$\Delta_1$	–
1	1	2	2	$(a, b)(c, d)$	$\Delta_2$	–
1	1	1	2	$(a, b, c)(d)$	$\Delta_3$	–
1	1	2	1	$(a, b, d)(c)$	–	–
1	1	2	3	$(a, b)(c)(d)$	$\Delta_4$	–
1	2	1	1	$(a, c, d)(b)$	$\Delta_5$	–
1	2	2	2	$(a)(b, c, d)$	–	–
1	2	3	3	$(a)(b)(c, d)$	$\Delta_6$	–
1	2	1	2	$(a, c)(b, d)$	$\Delta_7$	$\kappa_2$
1	2	2	1	$(a, d)(b, c)$	–	–
1	2	1	3	$(a, c)(b)(d)$	$\Delta_8$	$\kappa_1$
1	2	3	1	$(a, d)(b)(c)$	–	–
1	2	2	3	$(a)(b, c)(d)$	–	–
1	2	3	2	$(a)(b, d)(c)$	–	–
1	2	3	4	$(a)(b)(c)(d)$	$\Delta_9$	$\kappa_0$

## 2.1 Coefficient of identity by descent

Two-person relationships are compactly summarised in numerical form using the *coefficients of identity by descent* ( $\delta_i$ ) and *condensed coefficients of identity by descent* ( $\Delta_i$ ) of Jacquard (1974) (chapter 6), which are probabilities of particular patterns of identity by descent. The  $\delta_i$  are the probabilities for the 15 individual rows of Table 1, the  $\Delta_i$  those of the 9 subsets of genotypically equivalent states, where we do not keep track of which parent donates which allele. It is these condensed coefficients of identity that we use to characterise and quantify relationships among related individuals, including mixture contributors. Where inbreeding is ruled out,  $\Delta_i = 0$  for  $i = 1, 2, \dots, 6$ , and we need only the  $\kappa$  coefficients of Cotterman (1940):  $\kappa_0 \equiv \Delta_9, \kappa_1 \equiv \Delta_8, \kappa_2 \equiv \Delta_7$  are the probabilities that the two individuals share 0, 1 or 2 alleles by descent. As examples,

- (a) a parent and child have a relationship summarised by  $\kappa_0 = 0, \kappa_1 = 1, \kappa_2 = 0$ ,
- (b) two half-siblings (with unrelated parents) have  $\kappa_0 = 0.5, \kappa_1 = 0.5, \kappa_2 = 0$ , while
- (c) two children from an incestuous brother-sister mating are captured by  $\Delta = (0.06250, 0.03125, 0.12500, 0.03125, 0.12500, 0.03125, 0.21875, 0.31250, 0.06250)$ .

The  $\kappa$  and  $\Delta$  coefficients can be calculated from a pedigree by simple recursive calculations down the pedigree. In **R**, these are performed by the functions `kappaIBD` and `condensedIdentity`, respectively, in the package `ribd` (Vigeland 2019b), part of the `pedtools` family of packages created by Vigeland (2019a).

For more than 2 individuals, Thompson (1974) seems to have been first to provide a general framework for gene identity given multiple relationships. She provides a rigorous algebraic formalism, with particular attention to enumerating the intrinsic symmetries in the problem, and counts the numbers of possible relationships, which increase very rapidly. For example, for 4 individuals, there are 712 possible (genotypically equivalent) IBD states, reducing to 139 if inbreeding is ruled out. In typical pedigrees, only a very small fraction of these have positive probability, so the vast majority of condensed coefficients of identity are 0. We use what amounts to a sparse representation of such vectors of coefficients, namely a listing of which coefficients are non-zero, and their probability values; there are examples in Tables 2 and 3, where we use an arbitrary member of each equivalence class as a representative. We call this representative an IBD pattern and the whole table the IBD pattern distribution. These ‘multi-person condensed coefficients of identity’ can be calculated efficiently from a pedigree using a method devised with Magnus Dehli Vigeland; see function `pedigreeIBD` in the **R** package `KinMix`.

We can represent each IBD pattern in various ways. One is by a vector of integer labels, of length twice the number of individuals,  $n$ , say, the pair in entries  $(2i - 1, 2i)$  representing the genotype of the corresponding individual  $i = 1, 2, \dots, n$ . The numerical value of the labels is irrelevant, all that matters is whether two labels are the same or different, so the vector denotes a partition of the  $2n$  genes according to which are identical by descent. Since we are only concerned with unordered pairs of genes, the interpretation of the pattern is unchanged if elements  $(2i - 1, 2i)$  are exchanged, and also, of course, unchanged by any 1–1 relabelling. Diagrammatically, the pattern can be represented as a graph with  $2n$  vertices laid out in a  $n \times 2$  rectangular array, and vertices connected by an arc if the corresponding genes are identical by descent. Both representations of IBD patterns were used (with  $n = 2$ ) by Jacquard (1974) (chapter 6). Figure 2 and Table 3 show two examples of IBD pattern distributions in each of these representations.

As a foretaste of what can be done with the  $\kappa$  and  $\Delta$  coefficients, or their generalisation the IBD pattern distribution, we remark that, together with the population alleles frequencies, they determine the joint distribution of the genotypes for any set of individuals; as a simple example,

if  $a$ ,  $b$  and  $c$  are distinct alleles, with population frequencies  $q_a, q_b, q_c$ , and in the absence of inbreeding, the probability that two individuals have genotypes  $(a, b)$  and  $(a, c)$  respectively is simply  $\kappa_0(4q_a^2q_bq_c) + \kappa_1(q_aq_bq_c)$ , when their relationship is summarised by  $\kappa = (\kappa_0, \kappa_1, \kappa_2)$ . This can be verified directly algebraically with care, but in Section 3 we generalise this calculation and use it in modelling and analysing DNA mixtures.

## 2.2 IBD pattern distribution for a simple pedigree

As an illustration, consider a simple ‘triple’ of father F, mother M and child C, with the two parents unrelated. If we label the father’s genes by (1,2) and those of the mother by (3,4), then the child will have one gene that is either 1 or 2, and another gene that is 3 or 4; thus its genotype is (1,3), (2,3), (1,4) or (3,4) with equal probability. In tabular form, we could write this family’s genetic structure at any single autosomal locus in a table as in panel (a) of Table 2, where we have labelled the columns with the individual identities, and the rows with the corresponding probabilities.

Table 2: IBD pattern distributions for a Father/Mother/Child triple, F, M, C.

(a) Distinguishing maternal and paternal genes

pr	F	M	C
0.25	1	2	3
0.25	1	2	3
0.25	1	2	3
0.25	1	2	3

(b) Condensed form: Not distinguishing maternal and paternal genes

pr	F	M	C
1	1	3	2

(c) Extending the family to include the paternal grandfather

pr	F	M	C	GF
0.5	1	3	2	4
0.5	1	3	2	4

Note that separately in each row, we can arbitrarily permute the actual labels, so the first row of Table 2(a) could have been (2,4,1,3,2,1) without changing the meaning; the purpose of the labels is solely to indicate which genes are identical (by descent) and which different. Since a genotype is an *unordered* pair of genes, the interpretation of the table is also unchanged if any of the individual pairs are transposed, so the first row could equivalently be written (2,1,4,3,1,3), for example, and in many other ways. Combining these two rules, and aggregating the probabilities of identical rows, further economy of notation is possible: for example we could simply use the table in panel (b) of Table 2, to represent the same family, saving space and computer time. Effectively the labels 1 and 2 are then being used for the child’s paternal and maternal genes respectively.

The example can be extended, by, for example, including also the Father’s father, GF. There are two equally likely possibilities: the gene inherited by Father from his father might be that labelled 1 or 3. So the relationships between the 4 individuals can now be represented by panel (c) of Table 2.

### 2.3 Pairwise relationships do not determine joint relationships

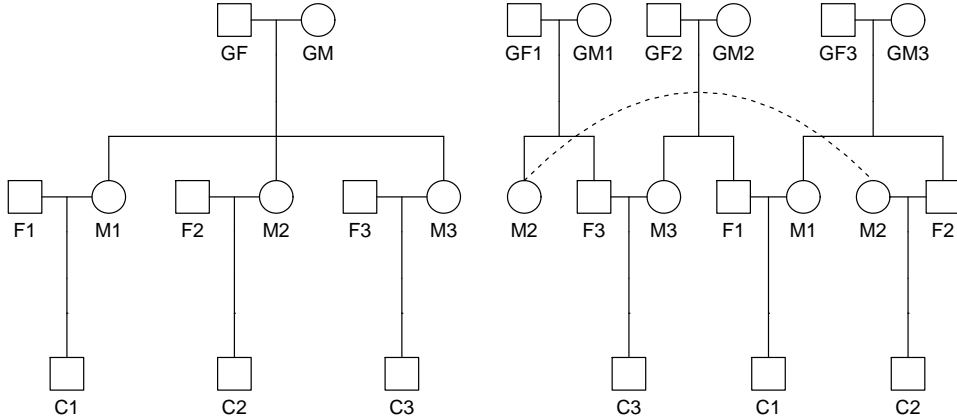


Figure 1: Pedigrees for the two 3-cousins scenarios: (left) star, (right) cyclic; one individual appears twice, to reduce line-crossing – the dotted curves link the replicate symbols.

To demonstrate that pairwise relationships do not determine a full description of relatedness among more than two individuals, even in the absence of inbreeding, we present the simplest example. Consider two scenarios in which among three individuals, each pair are full cousins, that is have  $(\kappa_0, \kappa_1, \kappa_2) = (0.75, 0.25, 0)$ . This can arise in a ‘star’ arrangement, where the three have mothers who are full siblings, but unrelated fathers (or vice-versa, of course). In a ‘cyclic’ arrangement, each pair of cousins have between them parents of the opposite sex who are siblings, with the other parents unrelated. The two pedigrees are displayed in Figure 1.

Table 3: IBD pattern distributions for two scenarios of 3 pairwise cousins; (left) star, (right) cyclic arrangements.

pr	C1	C2	C3	pr	C1	C2	C3						
0.3750	1	2	3	4	5	6	0.421875	1	2	3	4	5	6
0.1875	1	2	1	3	4	5	0.140625	1	2	1	3	4	5
0.1875	1	2	3	4	1	5	0.140625	1	2	3	4	1	5
0.1875	1	2	3	4	3	5	0.140625	1	2	3	4	3	5
0.0625	1	2	1	3	1	4	0.046875	1	2	1	3	2	4
							0.046875	1	2	1	3	3	4
							0.046875	1	2	3	4	1	3
							0.015625	1	2	1	3	2	3

The respective IBD pattern distributions are shown in Table 3 and visualised in Figure 2; the formats of each are described at the end of Section 2.1. It is very clear from these displays that these two families have different overall relatedness, for example in the star arrangement, there is probability 0.0625 that the three cousins have a common allele by IBD (as seen in the left-hand panels of Table 3 and Figure 2), while this is impossible in the cyclic arrangement. In Section 7, we include a simulation experiment demonstrating the extent to which these pedigrees can be

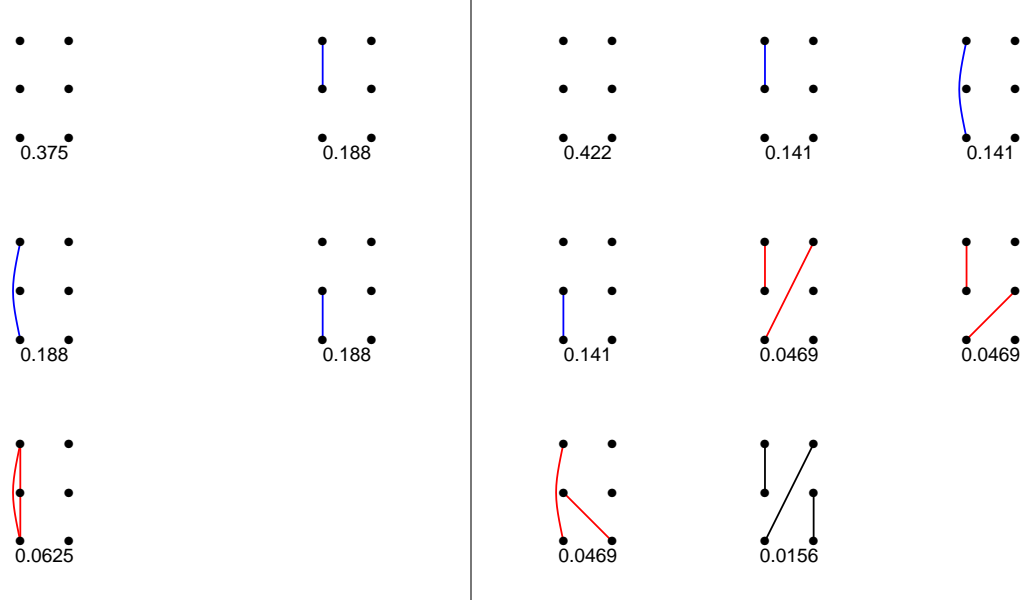


Figure 2: IBD pattern distributions for two scenarios of 3 pairwise cousins; (left) star, (right) cyclic arrangements. From top to bottom, the individuals are those labelled C1, C2 and C3, respectively, in Figure 1.

distinguished from DNA mixtures of STR markers with these family members as contributors.

## 2.4 IBD pattern distribution in the Iulius-Claudius pedigree

As a demonstration that the IBD pattern distribution among a handful of individuals can be readily computed even when the pedigree describing their relationships consists of as many as 35 individuals, and inbreeding is present, we briefly consider the Iulius-Claudius dynasty. This was the first Roman imperial dynasty, consisting of the first five emperors – Augustus, Tiberius, Caligula, Claudius, and Nero – and the family to which they belonged. They ruled the Roman Empire from its formation under Augustus in 27 BCE until 68 CE, when the last of the line, Nero, committed suicide. The name Iulius-Claudius dynasty refers to the two main branches of the imperial family: the gens Iulia and the gens Claudia. Figure 3 presents the Iulius-Claudius pedigree. Some of the names have been abbreviated.

As highlighted by the double horizontal bars in Figure 3, there are two inbred marriages within the pedigree, the first, between Germanicus and Agrippina Maior, leading to the other. The two emperors Caligula and Nero are descendants of this couple. We therefore look at the IBD pattern distribution among Germanicus, Agrippina Maior, Caligula and Nero, and also that between the three emperors Claudius, Caligula and Nero. Figure 4 shows excerpts (the most probable 9 patterns) of the IBD pattern distribution for these two subsets of individuals, respectively. As one can see from the figure, both Caligula and Nero share many alleles IBD. As an example of summarising a pairwise relationship, Germanicus and Agrippina Maior, parents of Caligula and of Nero's mother, have probabilities of sharing none and one of their genes IBD equal to  $\kappa_0 = 0.9375$  and  $\kappa_1 = 0.0625$ . The IBD pattern distribution, and coefficients like these extracted from it, very compactly yet exactly capture the very complex multi-generational story told by the pedigree.

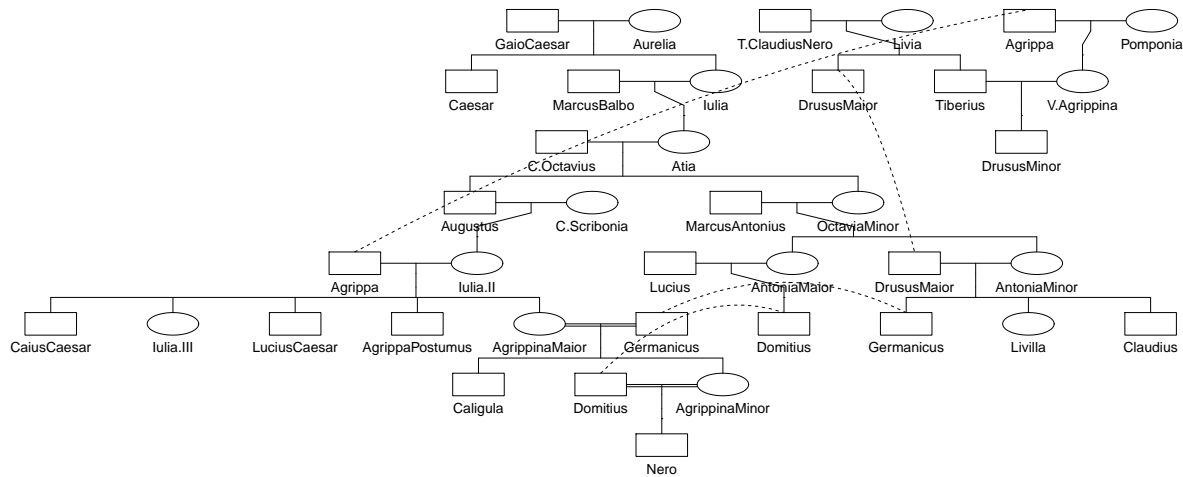


Figure 3: Iulius-Claudius family tree

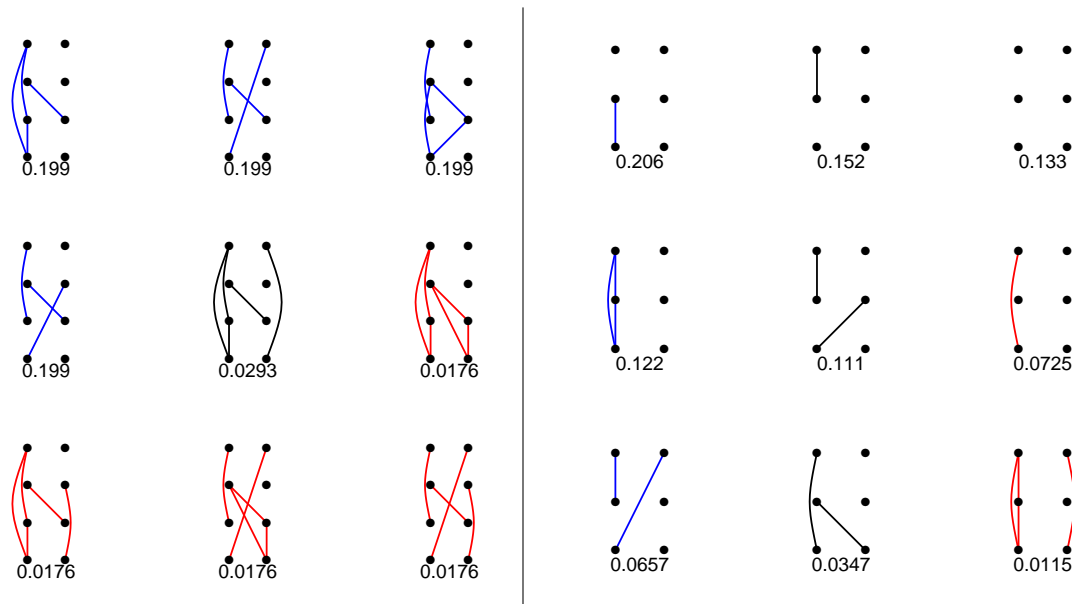


Figure 4: (left) Most probable patterns in the IBD pattern distributions for (respectively from the top) Germanicus, his wife Agrippina Maior and their descendants the Emperors Caligula and Nero, (right) the same for the three Emperors Claudius, Caligula and Nero.

### 3 Computations for DNA mixtures

#### 3.1 Likelihoods and Bayes nets

Under our universal assumption that we are using unlinked autosomal markers, and all individuals are drawn from a population in Hardy-Weinberg equilibrium, it is clear that genotypes  $\mathbf{n}$  and peak heights  $\mathbf{z}$  are independent across markers. Then the distributions  $p(\mathbf{n})$  and  $p(\mathbf{z}|\mathbf{n})$  are products over markers – and therefore so are likelihood ratios computed from them. We therefore consider each marker separately, and assume a single marker for the rest of this section. The likelihood for observed peak heights  $\mathbf{z}$  is of course

$$p(\mathbf{z}) = \sum_{\mathbf{n}} p(\mathbf{n})p(\mathbf{z}|\mathbf{n}), \quad (1)$$

regarded as a function of the parameters in the two model component distributions.

For the peak height model introduced and investigated by Cowell *et al.* (2015),  $p(\mathbf{z}|\mathbf{n})$  is defined as follows. As in Cowell *et al.* (2015) it is both convenient algebraically and vital computationally to represent genotypes  $\mathbf{n}$  by allele count arrays:  $n_{ia} = 0, 1, 2$  being the number of allele  $a$  in the genotype for individual  $i$ .

The peak heights  $Z_a$  at allele  $a$  are gamma distributed

$$Z_a \sim \Gamma \{ \rho D_a(\phi, \xi, \mathbf{n}), \eta \}, \quad (2)$$

independently for each  $a$ , where  $\eta$  denotes the scale (not rate),  $D_a(\phi, \xi, \mathbf{n}) = (1 - \xi) \sum_i \phi_i n_{ia} + \xi \sum_i \phi_i n_{i,a+1}$  the effective allele counts taking into account the stutter artefact and  $\phi = (\phi_i)_{i=1}^I$  denotes the proportion of DNA from individual  $i$  in the mixture.

For given genotypes  $\mathbf{n}$ , given parameters  $\psi = (\rho, \xi, \eta, \phi)$ , the conditional distribution for the peak heights  $\mathbf{z} = (z_a)_{a=1}^A$  factorizes over alleles  $a$

$$p(\mathbf{z}|\mathbf{n}) = p(\mathbf{z}|\mathbf{n}; \psi) = \prod_a L_a(z_a) \quad (3)$$

where

$$L_a(z_a) = \begin{cases} g\{z_a; \rho D_a(\phi, \xi, \mathbf{n}), \eta\} & \text{if } z_a > C \\ G\{C; \rho D_a(\phi, \xi, \mathbf{n}), \eta\} & \text{otherwise,} \end{cases}$$

with  $g$  and  $G$  denoting the gamma density and cdf respectively and  $C$  the detection threshold.

For a given hypothesis  $\mathcal{H}$  about the joint distribution  $p(\mathbf{n})$  of the genotypes of the  $I$  individuals, the full likelihood is obtained by summing over all possible combinations of genotypes to give  $p(\mathbf{z}) = p(\mathbf{z}; \psi)$  as in (1).

Unless both the number of mixture contributors and the number of alleles are very small, computing the sum in (1) is a formidable task, often an intractable one. The key observation in Graversen and Lauritzen (2015), exploited in the **DNAmixtures** package, is that if genotypes  $\mathbf{n}$  are encoded as allele count arrays ( $n_{ia}$ ) giving the number of alleles of type  $a$  for individual  $i$ , and the joint distribution  $p(\mathbf{n})$  factorised into conditional distributions sequentially over  $a$  for each  $i$ , then  $p(\mathbf{n})$  has the structure of a Bayes(ian) net(work) (BN) with considerable sparsity.

Computation of  $\sum_{\mathbf{n}} p(\mathbf{n})p(\mathbf{z}|\mathbf{n})$ , which is the expectation over the BN distribution for  $\mathbf{n}$  of the function  $p(\mathbf{z}|\mathbf{n})$ , is then exactly the kind of task performed by a BN probability propagation algorithm (Lauritzen and Spiegelhalter 1988). We follow the **DNAmixtures** formulation, including the allele count array representation of genotypes; for more computational detail see Graversen and Lauritzen (2015).

The IBD pattern distribution formulation helps to create methodology that considerably extends that described in Green and Mortera (2017). That paper introduced four approaches to adapting the Bayes net computation in `DNAmixtures` to deal with paternity testing (where the putative father is a contributor to the mixture, and with or without the mother’s genotype profile being available in addition to the child’s). Three of these: ALN (additional likelihood node), RPT (replace probability tables) and MBN (meiosis Bayesian network) involve modifying the Bayes net and are fast and essentially exact, the other, WLR (weighted likelihood ratio) is slow and approximate but easy to code.

It turns out that the RPT method is easiest to adapt to the case of relationships that are more complex or involve more contributors. This entails replacing the default genotype conditional probability tables (CPTs), representing independent multinomial draws from the gene pool, by tables that encode assumed relationships and condition on any observed genotypes. All genotypes are determined by the values of founding genes and the meiosis pattern, so by including founding genes and the meiosis pattern as nodes in the Bayes net, the CPTs for the individual genotype arrays consist only of 0’s and 1’s; they are then easy to construct, and can be stored compactly and processed efficiently.

Rather than define this process formally in the cumbersome and unilluminating algebra needed for generality, here we work through an example in detail. We begin by giving a constructive definition of the joint distribution of a family’s genotypes, using the IBD pattern distribution describing the family; this is useful in its own right, but it can also be used explicitly in simulating cases for testing purposes, and it also helps to motivate how we can construct CPTs for allele count arrays.

### 3.2 The joint distribution of genotype profiles when contributors are related

Consider the 4-individual family in Table 2(c). We see that the genotypes of the 4 individuals are determined by 5 founding alleles, labelled 1, 2, …, 5, corresponding to the distinct labels in that table, and a binary variable selecting one or other row of the table. For the marker in question, suppose the allele values are denoted  $a = 1, 2, \dots, A$ , with frequencies  $(q_a)$ . In fact, given 5 i.i.d. discrete random variables  $a_1, a_2, \dots, a_5$  each with distribution  $(q_a)$ , and a binary random variable  $s \in \{1, 3\}$  with probabilities  $\frac{1}{2}, \frac{1}{2}$ , independent of the  $(a_i)$ , we can copy indices from the table to write the 4 required genotypes as

$$\text{Fgt} = (a_1, a_3), \quad \text{Mgt} = (a_2, a_4), \quad \text{Cgt} = (a_1, a_2), \quad \text{GFgt} = (a_s, a_5).$$

To see how this can be expressed in allele count array form, note that a variable  $x$  taking values in  $\{1, 2, \dots, A\}$  can be represented as a vector of  $A$  binary variables  $(x_a)_{a=1}^A$ , with  $x_a = \delta_{xa}$  (using the Kronecker delta). Further, we have  $P(x_a = 1|x_1, x_2, \dots, x_{a-1}) = q_a^* = q_a / \sum_{b=1}^{a-1} q_b$  if  $\sum_{b=1}^{a-1} x_b = 0$ , 0 otherwise. This describes the way that the founding genes are coded; for the genotypes, where the alleles counts  $n_{ia}$  are 0, 1 or 2, we have simply that each count is deterministically the sum of two of the binary founding gene counts, appropriately chosen, rather than the conditional binomial distributions found in Cowell *et al.* (2015).

The general formulation should be clear from this example. Given the IBD pattern distribution, there will be a founding gene for each distinct label among the patterns, and the allelic values of these are drawn from the assumed population allele frequencies for the marker in question. A pattern is drawn from the IBD pattern distribution, and the genes and hence genotypes for all individuals obtained by selecting the corresponding founding gene values. The IBD pattern distribution applies equally for all markers, but the drawing of the founding allelic values and of the IBD pattern will be independent for each marker. The typical structure of the Bayes net representing this model when the founding genes and individual’s genotypes are represented by

allele count arrays is shown for a small example in Figure 5; in general the graph depends on the number of individuals in the family and the IBD pattern distribution. Pseudo-codes for this algorithm, viewed as a method for simulating genotypes for members of a family, and those of the next two sections are given in Supplementary information, Section 1, and all are implemented in open-source code in the `KinMix` package.

### 3.3 CPTs for related contributors

The case where no individuals are genotyped, so we are simply modelling family relationships among some or all of the mixture contributors is very straightforward. As in the previous section, we use the IBD pattern distribution directly. Continuing the example above, with the 4 individuals labelled  $i = 1, 2, 3, 4$ , the nodes of the required BN represent  $\{n_{ia}, i = 1, 2, 3, 4; a = 1, 2, \dots, A\}$ ,  $\{m_{ja}, j = 1, 2, 3, 4, 5; a = 1, 2, \dots, A\}$ ,  $\{T_{ja}, j = 1, 2, 3, 4, 5; a = 2, \dots, A - 1\}$ , and  $s$ . Here  $n_{ia} = 0, 1, 2$  is the number of alleles  $a$  for individual  $i$ ,  $m_{ja} = 0, 1$  the numbers of  $a$  for founding gene  $j$ , and the  $T$  are cumulative sums of the  $m$  (cumulative over  $a$ ). The algorithm again proceeds recursively down the edges of the Bayes net, but at each node, instead of generating an allele count, we compute its conditional distribution in the form of a conditional probability table.

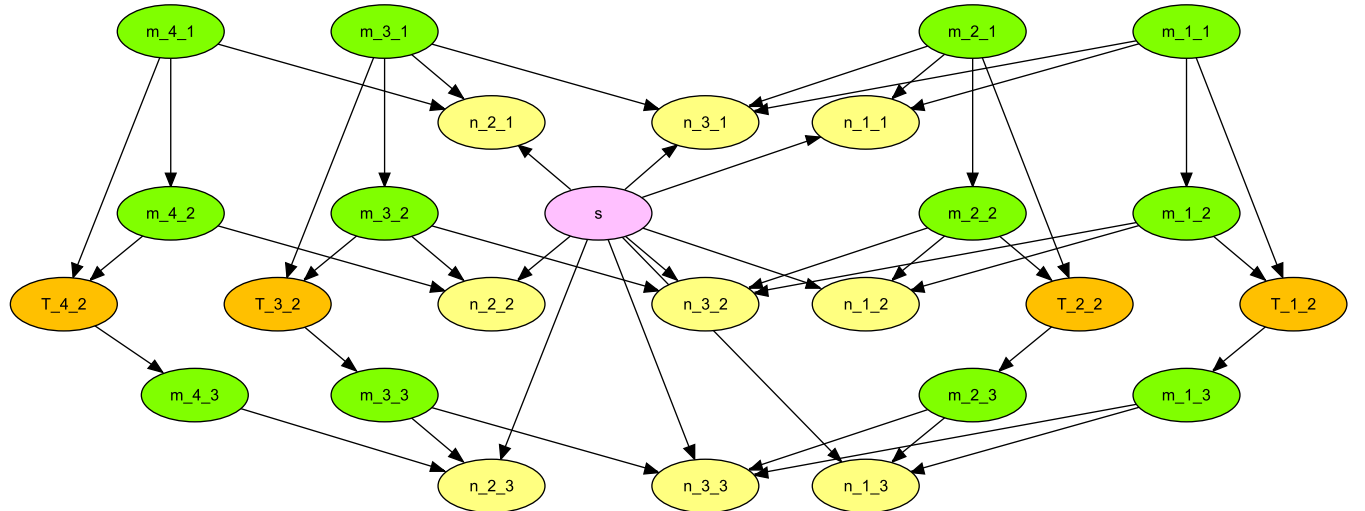


Figure 5: An example of the typical structure of a Bayes net for the joint distribution of several genotypes using the IBD pattern distribution: 3 genotypes derived from 4 founding genes, with 3 alleles. The node  $s$  represents the IBD pattern.

### 3.4 Conditioning on typed relatives

The case where some individuals in the family have been typed is a little more complicated; again similar reasoning applies to both simulation of genotypes, and computations of their CPTs.

Consider the 4-individual family again, and suppose that the Father and Mother are mixture contributors, and the Child and Grandfather are typed, with genotypes  $(a,b)$  and  $(b,c)$  respectively, where  $a, b$  and  $c$  are distinct alleles.

Our construction is shown schematically in Table 4. Recalling that genotypes are unordered pairs of genes, we first expand the IBD pattern distribution table by explicitly laying out all possible permutations of the allele labels for the two *typed* individuals, giving equal probability to each; this is to expedite checking for matches for each label. Matching these four allele labels onto their

Table 4: The worked example.

Fgt	Mgt	Cgt	GFgt	p(Cgt,GFgt)	Fgt	Mgt
1	<b>3</b>	2	<b>4</b>	1 2 1 5	0	
1	<b>3</b>	2	<b>4</b>	2 1 1 5	0.125 $q_a q_b q_c$	(b,?) (a,?)
1	<b>3</b>	2	<b>4</b>	1 2 5 1	0	
1	<b>3</b>	2	<b>4</b>	2 1 5 1	0	
1	3	2	<b>4</b>	1 2 3 5	0.125 $q_a q_b^2 q_c$	(a,b) (b,?)
1	3	2	<b>4</b>	2 1 3 5	0.125 $q_a q_b^2 q_c$	(b,b) (a,?)
1	3	2	<b>4</b>	1 2 5 3	0.125 $q_a q_b^2 q_c$	(a,c) (b,?)
1	3	2	<b>4</b>	2 1 5 3	0.125 $q_a q_b^2 q_c$	(b,c) (a,?)
				$a \neq b \neq c \neq a$		

observed values  $a,b,b,c$  respectively allows us to map allele labels onto actual allele values, for each of the permuted patterns. It also reveals that some permuted patterns cannot generate the observed alleles. For example the first row is impossible, given the observed genotypes, since the allele label 1 cannot simultaneously map onto the distinct alleles  $a$  and  $b$ , while the second row is possible, with the mapping  $1 \mapsto b$ ,  $2 \mapsto a$ ,  $5 \mapsto c$ . These mappings already determine some of the alleles of the Father and Mother, the mixture contributors. Those that are still not fixed are distinguished by underlining in bold in Table 4. A column has been added to the table giving for each permuted pattern the probability of the typed individuals having the observed values. The final columns for the table summarise what is now known about the Father's and Mothers' genotypes for each permuted pattern, with ? denoting a draw from the gene pool. (In this example, all such draws are independent, since there is no duplication in allele labels for the Father and Mother).

We now have all the information needed either to simulate Father and Mother genotypes, or to construct a Bayes net for the genotype allele count arrays of the Father and Mother, in each case conditional on the genotypes of the Child and Grandfather. The Bayes net 'parents' for each count node consist of one node indexing the permuted pattern, together with nodes indicating the values of the founding genes required. The probability distribution over the permuted pattern node is modified from the 'prior' (uniform) distribution by being conditioned on the typed genotypes, that is, it consists of the values of  $p(Cgt,GFgt)$  (see Table 4 in the case of our worked example), renormalised to sum to 1.

Table 5: A simpler example: simple paternity testing.

Fgt	Mgt	Cgt	p(Mgt,Cgt)	Fgt
1	<b>2</b>	3 4 1 3	0	
1	<b>2</b>	4 3 1 3	0	
1	<b>2</b>	3 4 3 1	0	
1	<b>2</b>	4 3 3 1	0.25 $q_a q_b q_c$	(c,?)
		$a \neq b \neq c \neq a$		

It might be useful to point out that the approach we take to computing conditional genotype probabilities (as a crucial step on the way to delivering likelihood ratios) avoids any manual algebra, which is straightforward in simple cases but can be tedious error-prone otherwise. Of course, it obtains the same answer. To see this, consider the familiar example of paternity testing given

both mother's and child's genotypes. For the case where these two genotypes are  $(a, b)$  and  $(b, c)$  respectively, where again  $a, b, c$  are all different, see Table 5, which is in exactly the same format as Table 4. Simple algebra tells us that the Father must donate the  $c$  allele, and that his other allele is drawn from the gene pool, and this is exactly the answer that Table 5 provides.

## 4 Ambient relatedness and uncertainty in allele frequencies

We have so far focussed on the role in modelling DNA mixtures of close relationships, specified through family structures. In this section, we will briefly touch on the different situation of what we will call *ambient relatedness*, that is where purportedly unrelated actors in fact have dependent genotypes because the population from which they are drawn exhibits high relatedness, for example through inbreeding. Just as with close relationships, these dependencies are driven by identity by descent, but the impact is somewhat different, both because it applies generally to the whole population, and because the dependence is usually substantially lower in magnitude.

In model-based inference from DNA profiles of STR markers, it has become routine to apply the ' $\theta$  correction' of Balding and Nichols (1994). The scalar parameter  $\theta$  can be identified with Wright's measure of interpopulation variation  $F_{ST}$  (Wright 1940; Wright 1951), and informally interpreted as the 'proportion of alleles that share a common ancestor in the same subpopulation'. As discussed by Balding and Nichols (1994), the parameter  $\theta$  arises in various models for dependent populations, for example the 'island model' of partially-separated sub-populations.

Green and Mortera (2009) observed that exactly the same probabilistic model for the joint distribution of multiple genes arises in a simple model for *uncertainty in allele frequencies* (UAF), in which the true allele frequencies are treated as unknowns with a Dirichlet distribution and the database used for calculation regarded as a multinomial sample from these true frequencies. The parameter  $\alpha = (1 - \theta)/\theta$  is then the effective size of the database. Green and Mortera (2009) also observed that this model is amenable to implementation as a Bayes net, as an alternative to algebraic specification; this Bayes net actually encodes a Pólya urn scheme.

### 4.1 Ambient IBD for allele count arrays

In discussion of Cowell *et al.* (2015), both Tvedebrink (modelling kinship) and Green (modelling uncertainty in allele frequencies) observe that when genotypes are represented by allele counts arrays  $n_{ia}$ , the number of alleles  $a$  of individual  $i$ , this Pólya urn scheme can be expressed through the recursion

$$\begin{aligned} n_{1.} &\sim \text{DM}(2, (\alpha_a)_{a=1}^A) \\ n_{i.} | (n_{j.})_{j=1}^{i-1} &\sim \text{DM}(2, (\alpha_a + n_{<i,a})_{a=1}^A) \end{aligned} \quad (4)$$

where  $n_{<i,a} = \sum_{j=1}^{i-1} n_{ja}$  (etc.), and DM denotes the Dirichlet–Multinomial distribution. See Green (2015); Tvedebrink (2010). The Dirichlet–multinomial distribution is the straightforward generalisation of the Beta–binomial to more than 2 categories. It is a Dirichlet mixture of multinomial distributions.  $X \sim \text{DM}(n, (\alpha_a)_{a=1}^A)$  means

$$P(X = x) = \left\{ \frac{n!}{\prod_a x_a!} \right\} \times \left\{ \prod_a \frac{\Gamma(\alpha_a + x_a)}{\Gamma(\alpha_a)} \right\} \times \frac{\Gamma(\sum_a \alpha_a)}{\Gamma(\sum_a \alpha_a + n)},$$

so long as  $\sum_a x_a = n$ .

Factorising the conditional distributions in (4) over alleles, we find that individual allele counts have Beta–Binomial conditional distributions:

$$n_{ia}|(n_{j.})_{j=1}^{i-1}, \{n_{ib}, b < a\} \sim \text{BB}((2 - n_{i,<a}), (\alpha_a + n_{i,a}), (\alpha_{>a} + n_{i,>a})).$$

The Beta–binomial distribution:  $X \sim \text{BB}(n, \alpha, \beta)$  means

$$p(X = x) = \binom{n}{x} \frac{\Gamma(\alpha + x)\Gamma(\beta + n - x)\Gamma(\alpha + \beta)}{\Gamma(\alpha)\Gamma(\beta)\Gamma(\alpha + \beta + n)}$$

Note that  $\text{BB}(1, \alpha, \beta)$  is just  $\text{Bernoulli}(\alpha/(\alpha + \beta))$ .

The `KinMix` package includes functions for modifying genotype CPTs to model UAF and ambient IBD.

Tvedebrink *et al.* (2015) give a fuller analysis, including a quantitative study of the implications. They show that relatedness/uncertainty in allele frequencies can *increase or decrease* LR’s in identification tasks.

## 4.2 UAF and IBD together

Particular casework may involve both close relationships and uncertainty in allele frequencies (or ambient relatedness). Modelling such a situation combines elements from Sections 3.3 and 4.1. Full details are omitted, but the key algebraic manipulations are given in Supplementary information, Section 2. The algorithmic implications are that Binomial distributions in algorithms would be replaced by Beta-Binomials, with the meiosis pattern as an additional parent at each instance of the Pólya urn. See also Cowell (2016) for a different analysis of this combined model.

At present, simultaneous modelling of close relationships and uncertainty in allele frequencies is not implemented in the `KinMix` package. Previous work with allele-presence data only (Green and Mortera 2009) and the work of Tvedebrink *et al.* (2015) show that the numerical difference in log likelihood ratios due to uncertainty in allele frequencies is rarely important in scientific terms.

## 5 Setting parameters

The methodology of this article is based on the joint probability model  $p(\mathbf{n}, \mathbf{z}) = p(\mathbf{n})p(\mathbf{z}|\mathbf{n})$  for the genotype profiles and peak heights, and this distribution has a number of parameters, notably the population allele frequencies, the relative proportions of the contributions of the different contributors to the mixture, and the parameters describing the PCR process and the artefacts of measurement embedded in the Cowell *et al.* (2015) peak height model. We do not prescribe any particular approach to setting these parameters when evaluating the likelihood, as this choice must be strongly influenced by regulation and practice in the judicial regime in which the analysis of the mixture is to be used, and the particular question that is being addressed.

Although Bayes nets are a key concept in the computations we use, this does not mean that a Bayesian formalism is intended. In fact the Cowell *et al.* (2015) model is presented as entirely frequentist, with the BN computations simply a device to compute an otherwise intractable likelihood function. The `DNAmixtures` package includes a function for maximising the likelihood as a function of the model parameters (the relative proportions of the contributions of the different contributors to the mixture, and the parameters describing the PCR process and the artefacts of measurement), and that function applies equally to a model modified using `KinMix`.

In principle a Bayesian analysis could be conducted, and the fast calculations of the likelihood that the packages provide would be an asset in implementing a Markov chain Monte Carlo (MCMC) sampler for posterior simulation, but we have not attempted this.

Considering now only maximum likelihood estimation (MLE), when we are comparing alternative models for mixtures, the question arises under which model(s) should the likelihood be maximised? The answer depends on context and perspective. In a likelihood ratio test of  $\mathcal{H}_p$  against  $\mathcal{H}_0$ , the respective likelihoods would each be maximised separately, and the ratio of the maximised values used as the test statistic. However, here the  $\log_{10} \text{LR}$  measures the weight of the evidence, and we are not appealing to statistical testing theory. In a criminal trial, depending on jurisdiction, custom might suggest or dictate choosing parameter values for both numerator and denominator that minimise the ratio, or perhaps maximise the denominator, in line with the presumption of innocence of the defendant (*in dubio pro reo*). In a civil case, say a paternity suit, the notion of defendant hardly applies.

Our experience has been that in many contexts, choice between these approaches makes little difference to the values of likelihood ratios, or their interpretations; we give a numerical example of this below. However, this cannot be a general conclusion; we anticipate, for example, that in comparing alternative hypotheses about the relatedness of mixture contributors to each other, parameter choice could have more impact.

Our numerical illustration revisits the Italian singer case, used for motivation in Green and Mortera (2017) (sections 4 and 5). This is a case of paternity testing, where the putative father is represented in the evidence only as a contributor to a mixture, assumed to be of 2 contributors, denoted  $U_1$  and  $U_2$ ; this is because the claim of paternity only arose some years after the putative father's death and the remains available had been corrupted. The child's genotype Cgt is available, and we presented weights of evidence for paternity, with and without using also the mother's genotype Mgt. The hypotheses are  $\mathcal{H}_p$ , that the major contributor to the mixture is the father, against  $\mathcal{H}_0$ , that neither contributor to the mixture is related to the child (or mother).

Table 6 illustrates that under either  $\mathcal{H}_0$  or  $\mathcal{H}_p$  the MLEs ( $\hat{\psi}_0, \hat{\psi}_p$ , respectively) of the parameters  $\psi = (\rho, \eta, \xi, \phi_{U1}, \phi_{U2})$  do not vary substantially, as mentioned above. Table 7 gives the likelihood ratios in favour of paternity without and with information on Cgt's mother's genotype Mgt: a) when using the MLEs computed under  $\mathcal{H}_0$  in both numerator and denominator of the LR (columns 2 and 3) and b) when using the MLEs computed separately under  $\mathcal{H}_p$  and  $\mathcal{H}_0$  (columns 4 and 5). Adopting a) or b) makes only immaterial differences to the LRs (less than 2%), in the context where the LR in favour of paternity is already more than 250,000, and including also the information about the mother's genotype increases this at least 500-fold.

Table 6: Maximum likelihood estimates in the Italian singer paternity case; the parameters are those in the Cowell *et al.* (2015) peak height model.

MLEs	$\rho$	$\eta$	$\xi$	$\phi_{U1}$	$\phi_{U2}$
$\mathcal{H}_0$ – baseline	0.718	1124	0.006643	0.9783	0.02166
$\mathcal{H}_p$ with Cgt known	0.745	1083	0.006527	0.9797	0.02034
$\mathcal{H}_p$ with Cgt & Mgt known	0.745	1083	0.006526	0.9797	0.02035

Table 7: Likelihood ratios and their logarithms, in the Italian singer paternity case

Likelihood ratios	$\psi_p = \psi_0 = \hat{\psi}_0(z)$		$\psi_p = \hat{\psi}_p, \psi_0 = \hat{\psi}_0$	
$\mathcal{H}_p$ vs. $\mathcal{H}_0$	LR	$\log_{10}(\text{LR})$	LR	$\log_{10}(\text{LR})$
with Cgt	266100	5.425	270100	5.432
with Cgt & Mgt known	$143.5 \times 10^6$	8.157	$145.7 \times 10^6$	8.163

## 6 Software: the KinMix package

The modelling and methods introduced in this paper form the basis for an **R** package **KinMix** (Green 2020a), that extends the package **DNAmixtures** (Graversen 2013). As with **DNAmixtures**, therefore, the package relies on the **Hugin** system for probabilistic expert systems, accessed via the **Rhugin** package. The model for peak heights given genotypes  $p(\mathbf{z}|\mathbf{n})$ , together with the treatment of artefacts such as drop-out and stutter, are exactly as in Cowell *et al.* (2015). The **KinMix** package provides functions for constructing IBD pattern distributions from pedigree information, and using these pattern distributions to modify the default **DNAmixtures** genotype profile distribution  $p(\mathbf{n})$  (in which untyped individuals are assumed unrelated draws from a specified gene pool), to allow for related contributors.

**KinMix** also provides facilities from simulating genotype profiles from groups of individuals with specified joint relationships, making graphical displays of joint relationships, and many other utilities. In addition to the package manual pages in standard **R** format, a tutorial user guide is available as Green (2020b).

**KinMix** inherits from **DNAmixtures** the representation of genotypes via allele count arrays, which is key to saving both computation time and computer memory, and allows the modelling of mixtures with as many as 5 or 6 untyped individuals. Although building in relationships between individuals does increase both time and space requirements, examples in this paper demonstrate that quite complex problems can be considered. Under standard assumptions, once parameters are fixed, likelihoods and likelihood ratios in our mixture models factorise over markers. Further, in the case of related contributors, logarithms of likelihoods and likelihood ratios are weighted averages of those obtained from the individual IBD patterns. The weights are the probabilities of the patterns, the posterior probabilities in the case where some of the relatives have been typed. An option in **KinMix** allows exploiting these facts, with the effect of considerably reducing the storage requirements when many markers are involved, since separate BNs are used for each marker/IBD pattern combination.

## 7 Simulations

In this section, we examine the performance of  $\log_{10}$ -likelihoods, based on the Cowell *et al.* (2015) model, at discriminating between different joint relationships, in a study using simulated electropherogram (EPG) and genotype data. Each simulated data set consists of genotype profiles generated from a prescribed ‘True’ model, using the generative model in Section 3.2; from each we generate artificial EPG data using the **pcrsim** (Hansson 2017) package, which simulates the DNA amplification process. These PCR simulations were based on using the AmpF $\ell$  STR<sup>TM</sup> SGM Plus<sup>TM</sup> PCR Amplification Kit, with the Norwegian SGM database, on 10 STR markers, together with Amelogenin, all available in **pcrsim**. The numbers of cells amplified varied from 200 to 25<sup>1</sup>,

The resulting data are analysed using **KinMix** (Green 2020a), under a variety of assumed models. In each case, we compute the log likelihood ratio against a baseline model that assumes the same number of unrelated contributors. In all examples, the focus of interest is on the  $\log_{10}$  LR from the peak height data *given* the stated available genotypes, that is, on the additional information about the question of interest attributable to the mixture data. These ratios are tabulated or graphed for a small number of replicates<sup>2</sup> of the PCR process, for each of a small number of independently generated genotype profiles, thus giving an idea of the variation attributable to these two sources. Parameters for the **DNAmixtures** peak height model are estimated by maximum likelihood using

<sup>1</sup>Other PCR parameters were as defined by the **pcrsim** command `simPCR(data=res, pcr.prob=1, pcr.cyc=28, vol.aliq=20, vol.pcr=50, sd.vol.pcr=1)`.

<sup>2</sup>These are independent identically distributed repeats of the PCR simulation, not replicates in the sense of DNA replication.

that package, assuming the appropriate number of unrelated contributors, estimated separately on each simulated EPG.

Each analysis in the following experiments involves specifying the true joint relationship between the actors involved, the hypothesised relationship(s), which of the actors contribute to the mixture, and which if any of the actors are genotyped.

### 7.1 Study 1: Two-way relationships

In this experiment, we study DNA mixtures with two contributors, and no other typed actors. We consider 5 possible familial relationships between the two contributors; for each relationship, we simulate EPG data and fit mixture models hypothesising each of the 5 relationships in turn. In Table 8, we report the median  $\log_{10}$  LR for each of the hypothesised models, over 4 replicated EPGs for each of 4 replicated genotypes. In each case the EPG data are simulated with 150 cells from the major contributor and 50 from the minor one.

Table 8: Study 1: Median  $\log_{10}$  LR over 4 replicated EPGs for each of 4 replicated genotypes, for 5 hypothesised models.

true	$\kappa_0$	$\kappa_1$	$\kappa_2$	hypothesised				
				parent-child	sibs	half-sibs	cousins	half-cousins
parent-child	0	1	0	2.360	1.927	1.873	1.129	0.636
sibs	0.25	0.5	0.25	-4.089	1.812	1.294	0.748	0.409
half-sibs	0.5	0.5	0	-22.508	-0.831	0.474	0.355	0.198
cousins	0.75	0.25	0	$-\infty$	-0.472	0.219	0.320	0.213
half-cousins	0.875	0.125	0	$-\infty$	-1.939	-0.607	-0.097	0.004

The variation in these  $\log_{10}$  LRs across replicate genotype profiles and EPGs is depicted in Figure 6. The rows of the figure correspond to the true relationships, and the columns to the 4 replicate genotype profiles. Within each panel we see a colour-coded diagram showing the variation in  $\log_{10}$  LR over the 4 EPG replicates. The  $\log_{10}$  LRs when parent-child is hypothesised are suppressed from the Figure as they take extreme values, as can be seen in the parent-child column of Table 8.

The highest median  $\log_{10}$  LRs are all found down the diagonal, so that if we select a model on the basis of the largest, then on average, we correctly identify the true model in all 5 cases. This is most pronounced when the true model is parent-child, a pattern that is perhaps to be expected given the  $\kappa$  coefficients, also tabulated in Table 8. Some of the other relationships are harder to distinguish. Also, recall that many relationships, like half-sibs, aunt/uncle, grandparent *etc.* have identical IBD pattern distributions and  $\kappa$  coefficients. Perhaps a more meaningful interpretation is that on an individual-replicate basis, for the 5 true relationships, in 11, 11, 9, 4 and 12 out of the  $16 = 4 \times 4$  replicates respectively, the correct model was identified.

When there is additional information, such as the genotypes of individuals potentially related to mixture contributors the evidence becomes much stronger, as we will see in some of the following examples.

### 7.2 Study 2: Three-way relationships

This experiment is exactly similar to the previous one, except now we consider relationships between 3 related contributors. The five considered relationships are respectively trio (mother, father and child); a mother and two children; 3 sibs; 3-cousins-cyclic, 3-cousins-star; the last two are defined and illustrated in Section 2.3. Again, there are no typed actors. In each case the EPG data are simulated with 100, 50 and 25 cells from the three contributors.

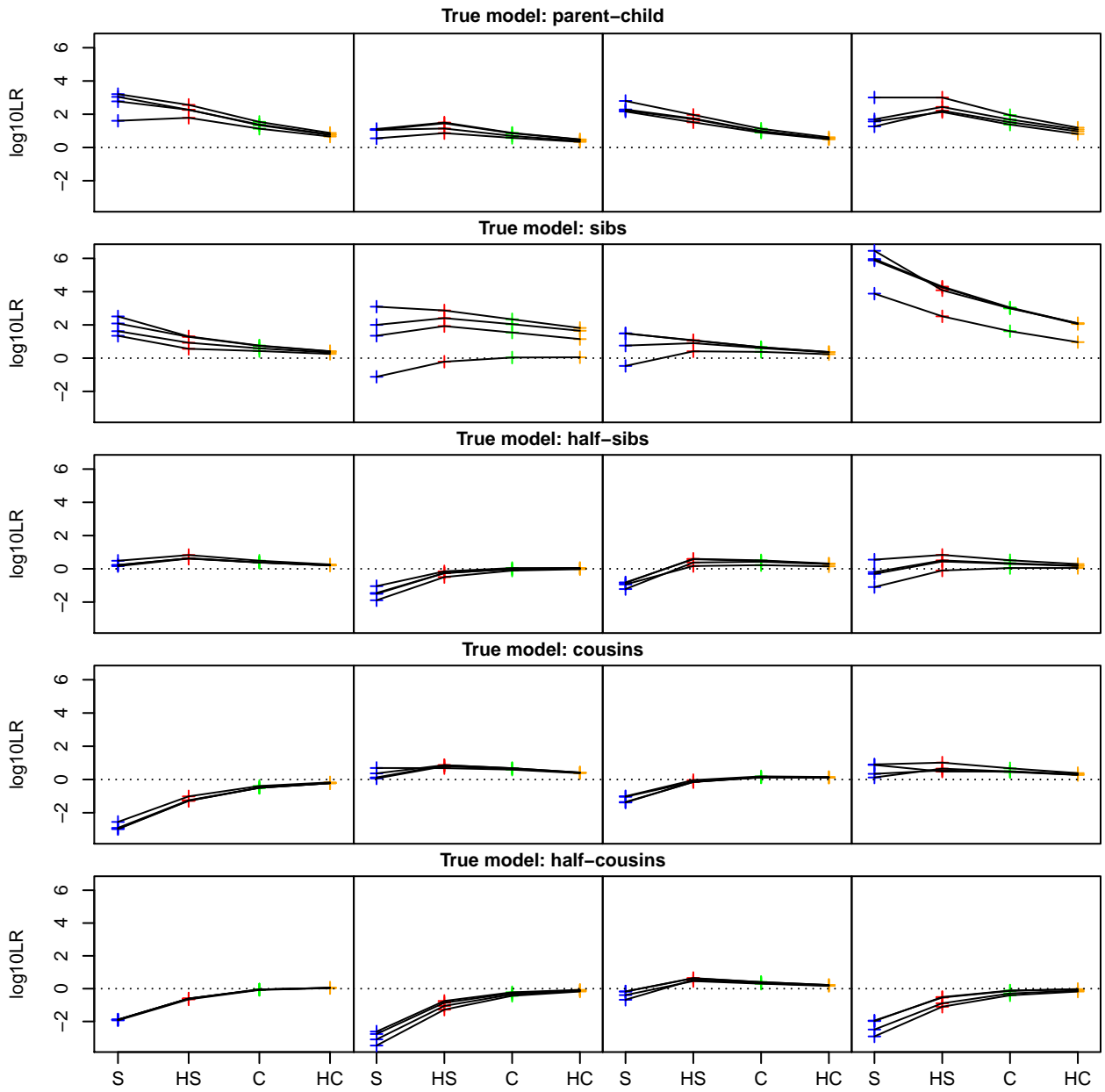


Figure 6: Study 1: Variation in the  $\log_{10}$  LRs across replicate genotype profiles and EPGs for the two-way example. The rows of the figure correspond to the true relationships, and the columns to the 4 replicate genotype profiles. Within each panel  $\log_{10}$  LR is plotted against hypothesised relationship (from left to right: sibs (S), half-sibs (HS), cousins (C) and half-cousins (HC), respectively). Lines join values corresponding to the same EPG replicate. The  $\log_{10}$  LRs when parent-child is hypothesised are suppressed from the Figure as they take extreme values, as can be seen in the parent-child column of Table 8.

Table 9: Study 2: Median  $\log_{10}$  LR over 4 replicated genotypes by 4 replicated EPGs in simulations of a DNA mixture for each 3-way relationship  $R$ .

true	hypothesised				
	trio	mother, 2 kids	3 sibs	3-cousins-cyclic	3-cousins-star
trio	2.772	−15.903	1.772	1.822	1.310
mother, 2 kids	2.032	5.280	4.260	2.929	2.230
3 sibs	−6.446	−3.800	3.584	2.417	1.917
3cousins-cyclic	−14.354	−20.380	−7.308	0.696	0.585
3cousins-star	−20.741	−20.325	−5.740	0.502	0.540

Table 9 gives the median  $\log_{10}$  LR relative to the baseline (three unrelated contributors) for comparing each combination of true and hypothesised relationship model, over 4 replicated genotypes by 4 replicated EPGs. The highest median  $\log_{10}$  LRs are again all found down the diagonal, implying that each of the 5 relationships are correctly identified on average. This effect is strongest when the relationships are mother and 2 children, or 3 sibs. In these two scenarios the 3 contributors all have a close pairwise relationship, whereas in the trio, the mother and father are unrelated. Also, the 3 cousins scenarios have more distant relationships among each other, and of course have identical pairwise relationships, so are harder to distinguish. These factors explain the asymmetry in the table. On a per-replicate basis, for the 5 true relationships, in respectively 12, 7, 12, 14, 11 out of the  $16 = 4 \times 4$  replicates, the correct model was identified.

Figure 7 shows the variation in  $\log_{10}$  LRs within the genotypes and across the 4 replicated EPGs in each row panel for 5 different 3-way relationships. As in the previous section, each row corresponds to a true relationship, and the four panels to the genotype profile replicates.

### 7.3 Study 3: Three-way relationships, with a relation genotyped

Here we consider 4 brothers, and DNA mixtures simulated from a true model in which three of the brothers are contributors. We consider testing  $\mathcal{H}_p$ : 3 brothers contributed to the mixture *vs.*  $\mathcal{H}_0$ : the 3 contributors are unrelated, and drawn from the gene pool. We perform this test with and without the assumption that the 4th brother is genotyped, yielding genotype  $Bgt$ , and as usual we generate 4 replicate joint genotype profiles, and 4 replicate EPGs for each. In each case the EPG data are simulated with 200, 100 and 50 cells from the three brothers contributing to the mixture; the same EPGs are used for the analyses without and with the 4th brother's genotype.

This kind of case can arise when brothers are engaged in a joint criminal activity and DNA might be found on, *e.g.* a get-away car, balaklava, banknote, crowbar, or gun.

The  $\log_{10}$  LR results are shown by replicate in Table 10 and Figure 8. Note that in most but not all of the  $16 = 4 \times 4$  replicates, there is much greater weight of evidence that the 3 brothers are in the mixture when the 4th brother's genotype is available.

### 7.4 Study 4: Incestuous sibs

Our remaining examples consider incestuous relationships in two person DNA mixtures of unknown or partly known contributors, in cases of possibly incestuous relationships. Unlike some other software, KinMix does handle incestuous relationships. This section concerns incest between sibs.

The setup we consider is of a father/mother/child trio, and a mixture where the contributors are the mother and child. Cases like this occur when a mother-foetus mixture is found and we wish to test the paternity. The hypotheses entertained are  $\mathcal{H}_p$  : the father and mother are siblings, as

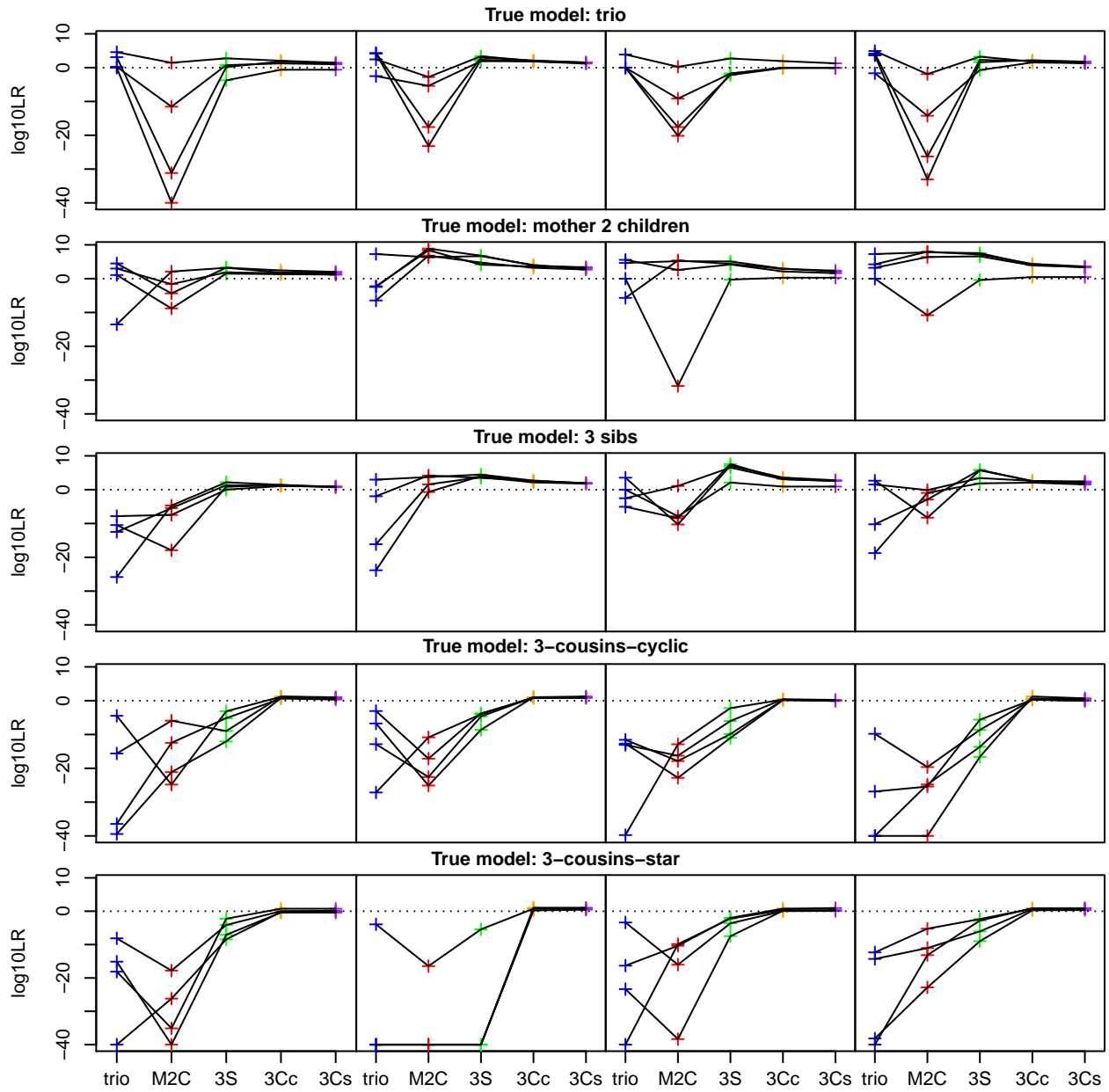


Figure 7: Study 2: Variation in the  $\log_{10}$  LRs across replicate genotype profiles and EPGs for the three-way example. The rows of the figure correspond to the true relationships, and the columns to the 4 replicate genotype profiles. Within each panel  $\log_{10}$  LR is plotted against hypothesised relationship (from left to right: trio, mother and two children (M2C), 3 sibs (3S), 3-cousins-cyclic (3Cc), 3-cousins-star (3Cs), respectively). Lines join values corresponding to the same EPG replicate. All values are truncated below at  $-40$  before plotting.

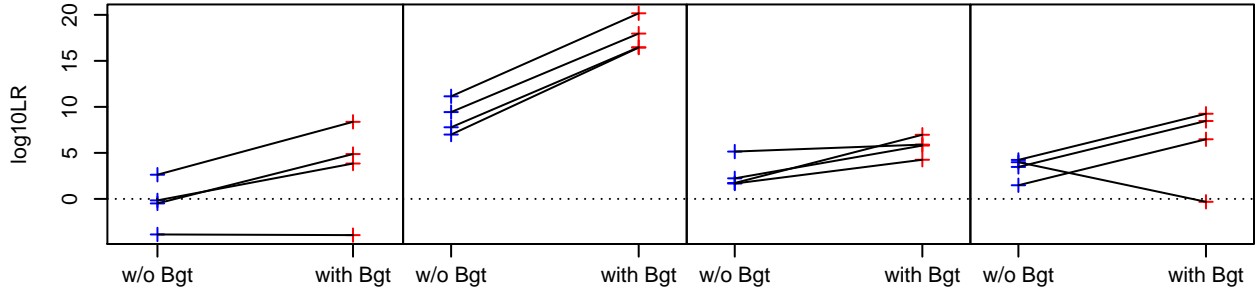


Figure 8: Study 3:  $\log_{10} \text{LR}$  for  $\mathcal{H}_p$  vs.  $\mathcal{H}_0$  in the case of 4 brothers, without and with the 4th brother genotyped. The 4 panels display results for the 4 replicate genotype profiles, the lines join results for the 4 replicate EPGs.

Table 10: Study 3: The contributors to a mixture are 3 sibs.  $\log_{10} \text{LR}$  for testing whether the contributors are 3 sibs or not, i.e.  $\mathcal{H}_p$ : 3 sibs contributed to the mixture vs.  $\mathcal{H}_0$ : the 3 contributors are unrelated. We also have the genotype Bgt of a 4th sib. The analysis is replicated  $4 \times 4$  times.

EPG replicate	without Bgt				with Bgt			
	genotype profile				genotype profile			
	1	2	3	4	1	2	3	4
1	-3.863	6.990	5.144	3.989	-3.936	16.442	5.899	-0.316
2	-0.489	11.146	2.235	1.483	4.874	20.166	5.796	6.480
3	2.630	9.434	1.731	4.236	8.375	17.964	6.967	9.251
4	-0.159	7.783	1.671	3.473	3.846	16.476	4.255	8.466

in the pedigree in Figure 9(a) and  $\mathcal{H}_0$  : the father and mother are unrelated. The EPG data are simulated under  $\mathcal{H}_p$  in this experiment, and with 200 cells from the mother and 100 from the child.

Table 11 shows the IBD pattern distribution of the three genotypes under  $\mathcal{H}_p$ .

Table 11: Sudy 4: IBD pattern for the incestuous case where the father F of the child C is the brother of the mother M.

pr	F	M	C
0.125	1	2	1
0.125	1	2	2
0.125	1	2	1
0.125	1	2	3
0.125	1	2	1
0.125	1	2	3
0.125	1	2	1
0.25	1	2	3
	4	1	3

The results for testing whether there was incest or not are shown in Table 12 and Figure 10, the table giving medians over the replicates, the figure showing the variation across  $4 \times 4$  replicates. In this example, there is very little variation across EPGs with genotype profiles.

Some of the dependency visible here on which actors are genotyped may seem counter-intuitive. For example, why does typing both Father and Child give apparently less clear evidence of incest than typing either one of Father and Child or neither separately, and indeed in some replicates

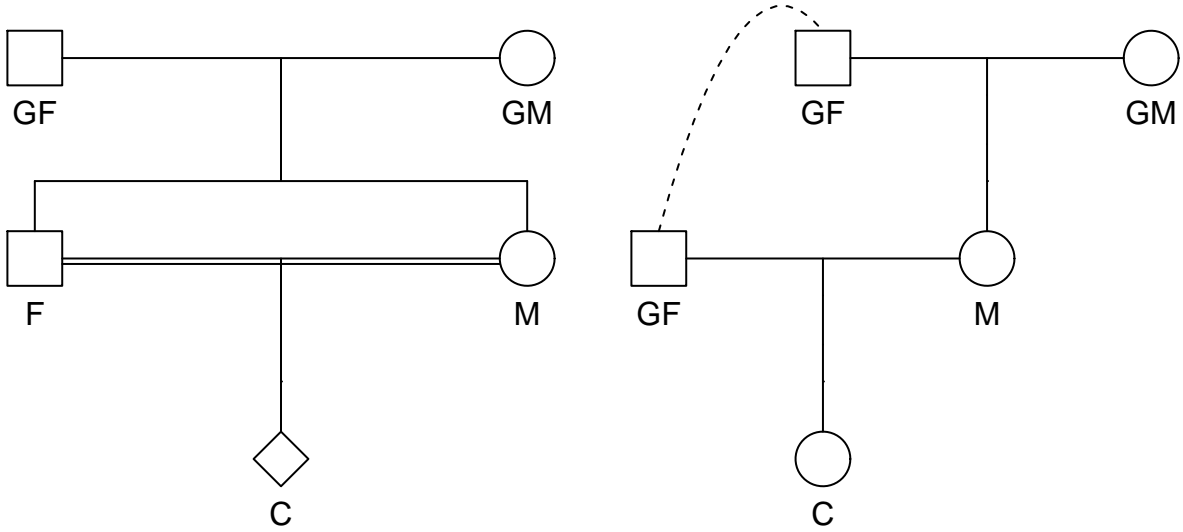


Figure 9: Studies 4 and 5: Pedigrees for ((a), left) incestuous sibs; ((b), right) father–child incest

give evidence against incest? Recall from the beginning of Section 7 that in all of our simulation studies, the focus of interest is on the  $\log_{10}$  LR from the peak height data *given* the stated available genotypes. Taking the peak height data and genotype data *together* (not shown here), as expected, removes the apparent paradox.

A more careful study of the conditional dependencies in this example reveals that the peak heights convey no information about incest if the Mother and one or other or both of the Father and Child are typed.

Table 12: Study 4:  $\log_{10}$  LR for testing whether there was incest or not, medians over  $4 \times 4$  replicate data sets.

	Typed actors				
	F & C	F	M	C	none
median $\log_{10}$ LR	1.030	2.718	1.233	0.076	1.318

## 7.5 Study 5: Incest and rape

Here we consider the horrendous scenario where a child has been raped, and we have a mixed trace from her vagina. The suspected culprit is her maternal grandfather, and additionally there is some suspicion that the grandfather is also her father, that is, that she is the offspring of an incestuous relationship between her mother and maternal grandfather. We assume the child is the major contributor to the mixture, and that there is one other contributor. The pedigree for the case of incest is shown in Figure 9(b), and this pedigree is assumed in simulating our EPG data for this study. The EPG data are simulated with 200 cells from the child and 100 from the rapist. In all cases we do not question that M is the mother of C, and that GF is the father of M. Table 13 shows the IBD pattern distribution of the three genotypes for an incestuous family where the maternal grandfather GF of a child C is the father of the mother M.

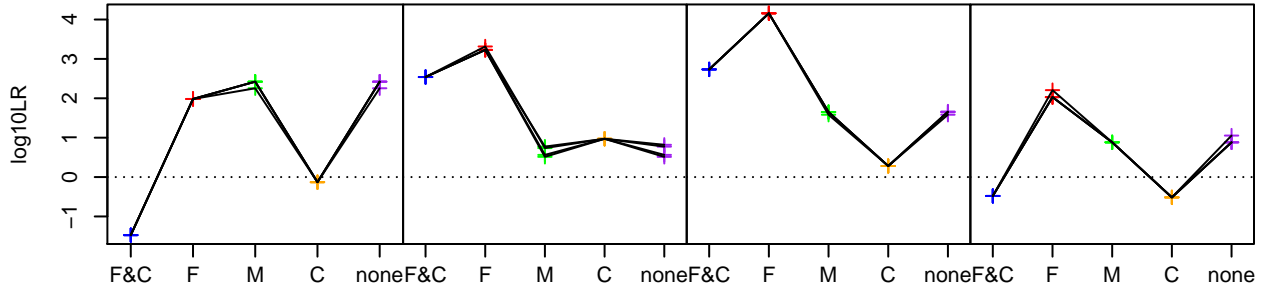


Figure 10: Study 4:  $\log_{10}$  LRs for the incestuous sibs example. The panels represent the replicated genotype profiles. In each panel, variation in  $\log_{10}$  LRs is shown across replicated EPGs, colour-coded by which actors are genotyped: dark blue, red, green, orange and purple for F, GF, M, C and none, respectively.

Table 13: Study 5: IBD pattern distribution for the incestuous case where the grandfather GF of a child C is the father of the mother M.

pr	GF	M	C
0.25	1	2	1
0.25	1	2	3
0.25	1	2	1
0.25	1	2	3

We consider various possibilities for which actors are separately genotyped: either both M and C, M only, C only, none. As before, our experiments for the above scenarios are based on 4 replicated genotypes by 4 replicated EPGs.

For brevity, in describing this study we will use the term *rape* to mean that the GF is the 2nd contributor to the mixture, and *incest* to mean that GF is father of C. We wish to examine whether it is possible from the DNA mixture and any typed genotypes to distinguish the possibilities of incest and/or rape. Table 14 reports the  $\log_{10}$  LRs for each of (i) rape assuming incest, (ii) incest assuming rape, (iii) rape assuming no incest, and (iv) incest assuming no rape. Figure 11 shows the variation in the  $\log_{10}$  LRs by replicate.

Note that for the test of incest assuming no rape, when the child's genotype is known, a conditional independence argument confirms that the  $\log_{10}$  LR is identically 0.

Table 14: Study 5:  $\log_{10}$  LRs for the tests (i)-(iv) over 4 replicated genotypes by 4 replicated epgs with the set of typed actors given in (b).

scenarios	typed			
	both M and C	M	C	none
rape assuming incest	25.145	7.713	20.403	3.679
incest assuming rape	2.916	4.608	1.721	2.506
rape assuming no incest	21.404	3.111	18.682	2.002
incest assuming no rape	0	0.574	0	0.787

We can see that there tends to be a stronger signal for rape than for incest, and also that when we have the additional information on the child's genotype the  $\log_{10}$  LR becomes much larger.

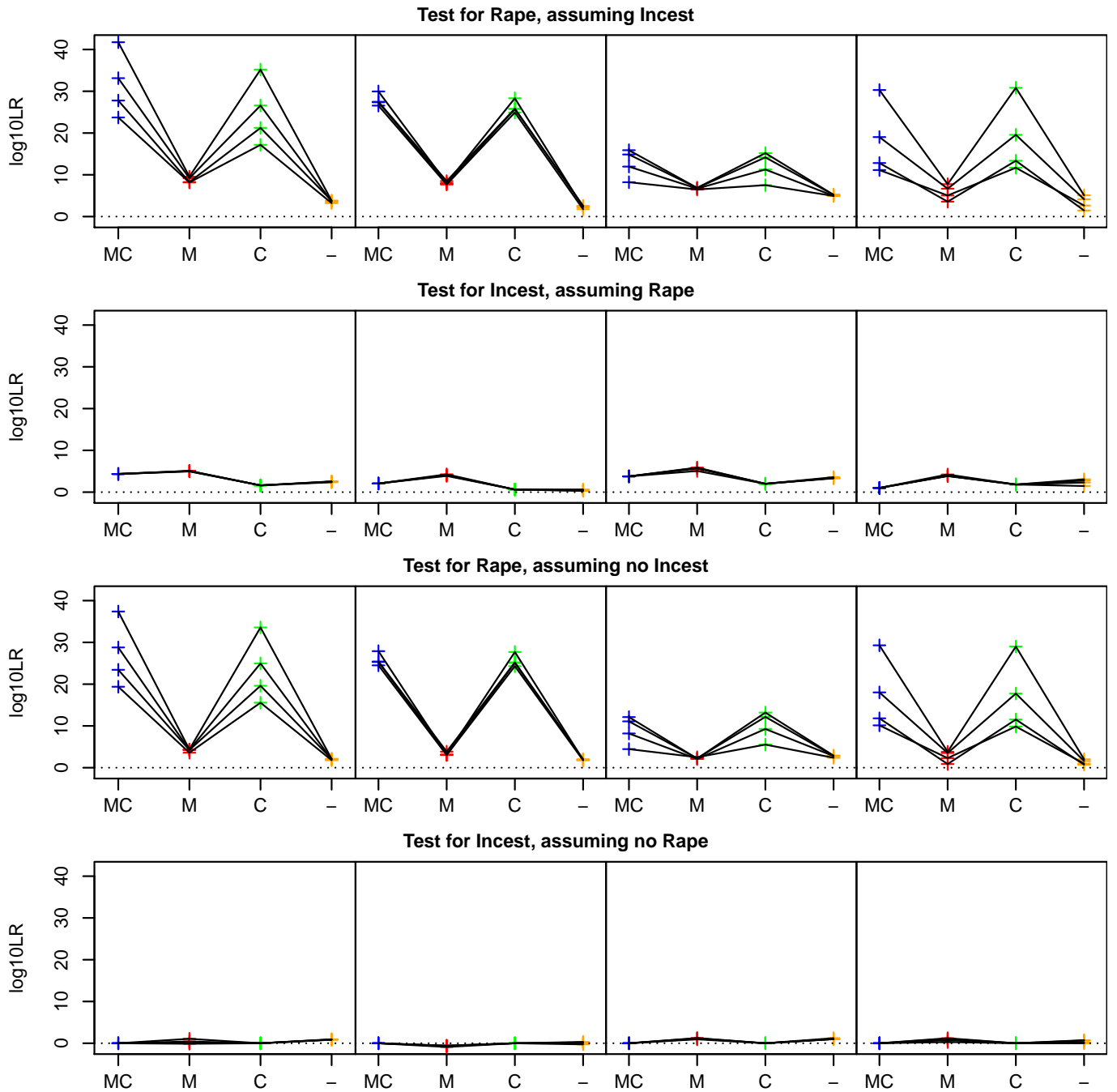


Figure 11: Study 5: Variation in the  $\log_{10}$  LRs across replicate genotype profiles and EPGs for the incest and rape example. The rows of the figure correspond to the various tests, and the columns to the 4 replicate genotype profiles. Within each panel  $\log_{10}$  LR is plotted against which actors are genotyped (colour-coded: blue, red, green, and orange for mother and child, mother alone, child alone, or no one, respectively). Lines join values corresponding to the same EPG replicate.

Having only the mother's genotype does not make a substantial difference.

## 8 Real case applications

### 8.1 Case 1: Identification of a missing person

Here we analyse a real case related to a missing male, provided by the DNA Laboratory, Comisaría General de Policía Científica of Madrid. We refer to Green *et al.* (2020) for full details of the case analysis. Here we will revisit some of the results, and also compare them with an analysis made with a different software.

In this case, only a daughter of the missing male was available to donate a DNA sample. A biological sample was collected from a toothbrush, presumably used by the missing person. DNA was recovered and analysed on 21 STR markers, plus three sex-related markers, included in GlobalFiler™ PCR amplification kit (ThermoFisher). The reference sample from the daughter of the missing male was also genotyped with the same kit. A two-person DNA mixture was detected on the toothbrush. We denote the two distinct unknown contributors by  $U_1$  for the major contributor and  $U_2$  for the minor. An excerpt of the data is shown in Table 15, showing the alleles and peak heights in the DNA mixture found on the toothbrush  $T$ . The DNA profile of the daughter, denoted by  $D$ , is also shown. The sex-related markers (not shown) indicated that the mixture was most probably from one male and one female donor.

Table 15: Case 1: An excerpt of the DNA mixture data from the toothbrush  $T$ , showing the markers, alleles and relative peak heights together with the daughter's genotype  $D$ .

markers	alleles	toothbrush	
		peak height	D
CSF1PO	10	1152	
	11	126	
	12	941	12
D22S1045	11	3218	
	15	3550	15
	16		
D5S818	11	5158	11
	13	304	13
vWA	14		
	16	264	16
	18	3664	18

Here we analyse the DNA mixture found on the toothbrush  $T$  presumed used by the missing person. We assume known allele frequencies taken from the Spanish allele frequency database collected on  $n = 284$  individuals (García *et al.* 2012). In all the analyses presented we adopt a threshold of 50 rfus (relative fluorescent units).

In the preliminary analysis of the data we found that the estimated proportion of DNA for the major contributor  $U_1$ ,  $\phi_{U_1} = 0.93$  is large. We also computed the  $\log_{10} LR$  for testing  $\mathcal{H}_p$ :  $D$  is the child of  $U_1$  (and similarly for  $U_2$ ) *vs.*  $\mathcal{H}_0$ :  $U_1$  and  $U_2$  are assumed drawn at random from the gene pool. As seen in the final row of Table 18, The  $\log_{10} LR = 10.97$  is large, pointing to  $U_1$  being a parent of  $D$  but it is also substantial,  $\log_{10} LR = 4.53$ , for the hypothesis that the minor contributor  $U_2$  is a parent of  $D$ . We then questioned whether  $U_1$  and  $U_2$  were possibly related. The negative  $\log_{10} LR$  for comparing  $\mathcal{H}_p$ :  $U_1$  has relationship  $R$  to  $U_2$ , *vs.*  $\mathcal{H}_0$ :  $U_1$  and  $U_2$  are unrelated, given

in Table 16, show that they are most likely to be unrelated and thus are likely to be the parents of D. Furthermore, the likelihood that D was one of the mixture contributors is practically zero.

Table 16: Casel:  $\log_{10}$  LR for  $\mathcal{H}_p$ :  $U_1$  has relationship  $R$  to  $U_2$ , vs.  $\mathcal{H}_0$ :  $U_1$  and  $U_2$  are unrelated.

Relationship $R$ between $U_1$ and $U_2$ under $\mathcal{H}_p$	$\log_{10}$ LR
parent-child	-15.54
sibs	-2.14
half-sibs	-0.37

Table 17 shows the  $\log_{10}$  LR for several hypotheses  $\mathcal{H}_p$  concerning different relationships  $R$  among  $U_1$ ,  $U_2$  and D, vs. two possible alternative hypotheses. The first alternative hypothesis is  $\mathcal{H}_1$ :  $U_2$  is a parent of D and  $U_1$  is unrelated. The second alternative hypothesis is  $\mathcal{H}_0$ : the two mixture contributors  $U_1$  and  $U_2$  are unrelated to D and to each other. The values of the  $\log_{10}$  LR show that it is likely that the two contributors are the missing father of D and D's mother. We also computed the weights of evidence when the roles of  $U_1$  and  $U_2$  are exchanged obtaining, for example, a smaller  $\log_{10}$  LR = 6.96 in place of the first value  $\log_{10}$  LR = 13.4 in Table 17. It thus seemed more likely that the mother is the major contributor  $U_1$  and the father is the minor contributor  $U_2$  than viceversa.

Table 17: Case 1:  $\log_{10}$  LR for several hypotheses  $\mathcal{H}_p$  concerning different relationships  $R$  among  $U_1$ ,  $U_2$  and D, vs.  $\mathcal{H}_1$ :  $U_2$  is the father of D and  $U_1$  was unrelated and  $\mathcal{H}_0$ : the two mixture contributors  $U_1$  and  $U_2$  are unrelated.

$\mathcal{H}_p$	$\mathcal{H}_1$	$\mathcal{H}_0$
$U_2$ father and $U_1$ mother of D	13.404	17.935
$U_2$ father of D and $U_1$ maternal aunt of D	11.049	15.579
$U_2$ father of D and $U_1$ paternal cousin of D	6.069	10.600
$U_2$ sib of $U_1$ and father of D	4.303	8.834
$U_2$ father of both D and $U_1$	-4.547	-0.016

### 8.1.1 Case 1, comparison with `relMix`

The R package `relMix` (Hernandis *et al.* 2019) also analyses DNA mixtures involving relatives, but is based only on allele presence, not considering the peak heights when modelling the DNA mixture as does `KinMix`. Based on the toothbrush sample, here we draw a comparison between results when using `KinMix` with and without the peak height data, and using `relMix`.

Table 18 presents a marker-wise comparison between the likelihood LR and the overall  $\log_{10}$  LR, for comparing  $\mathcal{H}_p$ :  $U_1$  is a parent of D vs.  $\mathcal{H}_0$ :  $U_1$  and  $U_2$  are assumed drawn at random from the gene pool. Note that on comparing columns 2 and 3 to column 4 in Table 18, for only 2 markers out of 20 does using the peak heights yield a smaller  $\log_{10}$  LR than using allele-presence data alone. The results obtained with `relMix` and `KinMix` when not including the peak height information are quite similar, although based on different models. As seen in the final row of Table 18, the overall  $\log_{10}$  LR on all the markers computed by `KinMix`, with peak heights, is 10.97, compared with the result 9.53 when not using the peak height information, a LR 27.5 times smaller.

We found that `relMix` was not able to compute the LR when there are more than 16 different alleles on a marker in the allele frequency database, as is the case for markers D12S391 and SE33. We indicate this in Table 18 by NaN. When using only the markers that `relMix` is able to compute,

Table 18: Case 1: Marker-wise LR and overall  $\log_{10}$  LR for item  $T$ , using **relMix** and **KinMix** with and without peak height information, for testing whether in  $T$ ,  $\mathcal{H}_p$ :  $U_1$  is a parent of D *vs.*  $\mathcal{H}_0$ :  $U_1$  and  $U_2$  are random members of the population.

marker	<b>relMix</b>	<b>KinMix</b> w/o peak heights	<b>KinMix</b> with peak heights
CSF1PO	1.08	1.07	1.59
D10S1248	1.26	1.18	1.62
D12S391	NaN	2.34	2.15
D13S317	3.02	3.11	4.84
D16S539	3.54	3.61	3.72
D18S51	4.75	4.93	5.16
D19S433	1.71	1.71	1.99
D1S1656	5.02	5.24	6.17
D21S11	1.89	1.74	2.39
D22S1045	1.60	1.49	1.23
D2S1338	9.23	9.81	12.89
D3S1358	2.25	2.26	2.27
D5S818	2.09	2.12	1.51
D7S820	7.18	7.77	10.92
D8S1179	3.48	3.52	6.77
FGA	6.30	6.35	10.92
SE33	NaN	5.53	5.07
TH01	2.39	2.46	2.54
TPOX	3.01	3.11	3.30
vWA	2.55	2.58	3.34
partial $\log_{10}$ LR	8.35	8.42	9.94
computation times (s)	1698	2.28	1.38 (2.38)
overall $\log_{10}$ LR		9.53	10.97

the partial  $\log_{10}$  LR obtained with **KinMix** with peak height information, is 9.94, is again substantially bigger than that obtained without peak height information (8.35 with **relMix**, 8.42 with **KinMix**).

The time to do the computations with **relMix** is considerably longer; it takes 1,698 seconds (almost half an hour) compared to 2.28 seconds for **KinMix** without peak height information, and the 1.38 seconds that **KinMix** takes using peak heights. (These times were obtained with an i7-7600U processor clocked at 2.80GHz.) This discrepancy between computational times is likely to be due to the fact that **KinMix** represents relationships in a DNA mixture in a compact and time-efficient way by representing genotypes using a Markov structure in a Bayesian network, so that computations can be done linearly in number of alleles. On the other hand, **relMix** explicitly enumerates all possible combinations of alleles which is a combinatorially intensive computational task.

## 8.2 Case 2: Rape case

Here we analyse another real case from the DNA Laboratory, Comisaría General de Policía Científica of Madrid, concerning a sexual assault. The victim stated that 2 individuals raped her, both using condoms. The two condoms were found and two DNA mixtures, EPG1 and EPG2, were detected and analysed on 22 markers including Amelogenin (for gender identification). The two

DNA mixtures were each compatible with the victim's profile and with that of an unknown male. An excerpt of the data on two DNA mixtures EPG1, EPG2 showing the markers, alleles, peak heights and victim's genotype is shown in Table 19.

Table 19: Case 2: An excerpt of the data on two DNA mixtures EPG1, EPG2 showing the markers, alleles, peak heights and victim's genotype.

marker	allele	EPG1	EPG2	victim
		height	height	
CSF1PO	10	1449	173	10
	11	133	129	
D10S1248	13	6380	1527	13
	14	1012	139	
D12S391	19	172		
	20	1001	152	20
D18S51	21	1193	73	21
	12		88	
	14	363		
	15	791	271	15
	16	1469	232	16
	19	461		

The police wished to know if the unknown male in EPG1 and that in EPG2 could belong to 2 brothers. We also tested whether the two unknown males have a relationship  $R = \{\text{father-son, brothers, half-brothers, cousins, or are identical (the same individual or a hypothetical monozygotic twin)}\}$ .

In order to deal with problems like this we consider having the victim,  $v$ , and two unknown contributor  $U_1$  and  $U_2$  in EPG1 and EPG2, and assume that the proportion contributed to EPG1 by  $U_2$  is  $\phi_{U_2} = 0$  and the proportion contributed to EPG2 by  $U_1$  is  $\phi_{U_1} = 0$ . The estimated mixture parameters for EPG1 and EPG2, under the above assumption, are given in Table 20.

Table 20: Case 2: Estimated parameters for EPG1 and EPG2 assuming they contain DNA from the victim  $v$  and two unknown contributor  $U_1$  and  $U_2$ . We assume that the proportion contributed to EPG1 by  $U_2$  is zero,  $\phi_{U_2} = 0$ , and the proportion contributed to EPG2 by  $U_1$  is zero,  $\phi_{U_1} = 0$ .

	$\rho$	$\eta$	$\xi$	$\phi_{U_1}$	$\phi_{U_2}$	$\phi_v$
EPG1	4.786	432.7	0	0.179	0	0.821
EPG2	1.996	289.9	0.0303	0	0.336	0.664

Table 21: Case 2:  $\log_{10}$  LR for testing  $\mathcal{H}_p : U_1$  in EPG1 and  $U_2$  in EPG2 have relationship relationships  $R$ , vs.  $\mathcal{H}_0 : U_1$  in EPG1 and  $U_2$  in EPG2 are unrelated. In both  $\mathcal{H}_p$  and  $\mathcal{H}_0$  we assume that the victim is a contributor to both EPG1 and EPG2.

	identity	father-son	brothers	half-brothers	cousins
relationship	2.36	2.60	2.48	2.56	1.84

Table 21 gives the  $\log_{10}$  LR for testing  $\mathcal{H}_p : U_1$  in EPG1 and  $U_2$  in EPG2 have relationship  $R$ , vs.  $\mathcal{H}_0$  : all contributors unrelated, except for the victim's presence in both. The  $\log_{10}$  LR points to there being a relationship between  $U_1$  and  $U_2$ . In particular, the  $\log_{10}$  LR = 2.48 that they are brothers rather than unrelated.

In subsequent developments of the case two brothers were arrested and DNA reference samples were collected from them. We compared the prosecution hypothesis  $\mathcal{H}_p : v$  and brother 1 contributed to EPG1 *vs.*  $\mathcal{H}_0 : v$  and an unknown, selected at random from the database, contributed to EPG1. The resulting  $\log_{10} \text{LR} = 22.28$  for  $\mathcal{H}_p \text{ vs. } \mathcal{H}_0$  is highly incriminating for brother 1. Similarly, when testing the prosecution hypothesis  $\mathcal{H}_p : v$  and brother 2 contributed to EPG2 *vs.*  $\mathcal{H}_0 : v$  and an unknown, selected at random from the database, contributed to EPG2, the  $\log_{10} \text{LR} = 24.14$  for  $\mathcal{H}_p \text{ vs. } \mathcal{H}_0$  is highly incriminating also for brother 2.

## 9 Discussion

We have shown that the IBD pattern distribution for a collection of related individuals, which extends Jacquard's concept of coefficient of identity by descent beyond pairwise relationships, is an invaluable approach both to encoding relationships and to Bayes net computations for DNA mixture analysis involving family relationships. Implementation of these ideas in the package `KinMix`, extending `DNAmixtures`, provides a convenient, powerful and flexible means for delivering the computations needed for DNA mixture analysis, using peak heights, involving arbitrarily complex relationships.

In this paper, we have not paid attention to the possibility of mutation, which can be important, for example in paternity cases, where a putative father can be excluded because his genotype profile is incompatible, even though a single mutation could make it compatible. We have experimental additions to `KinMix`, that compute likelihood ratios allowing for mutation, in various scenarios involving very close relationships. We aim to provide a comprehensive treatment of mutation in subsequent work.

## Acknowledgements

We thank Amke Caliebe, Thore Egeland and Michael Nothnagel for organising an excellent workshop on Advanced Statistical and Stochastic Methods in Forensic Genetics, in Cologne in August 2018, and acknowledge fruitful conversations with Marjan Sjerps, Nuala Sheehan, Torben Tvedebrink, and Magnus Dehli Vigeland at and after the meeting, and also helpful correspondence with Elizabeth Thompson, and comments from Phil Dawid. Oskar Hansson was very helpful in discussion about using his package `pcrsim`. We also thank Lourdes Prieto, Comisaría General de Policía Científica, DNA Laboratory, Madrid, Spain for providing the data for the real case applications.

Finally, we are indebted to the referees for their careful reviews, which have led to a much improved presentation of these ideas.

## References

- Balding, D. J. (2005). *Weight-of-Evidence for Forensic DNA Profiles*. Wiley, New York.
- Balding, D. J. and Nichols, R. A. (1994). DNA profile match probability calculation: How to allow for population stratification, relatedness, database selection and single bands. *Forensic Science International*, **64**, 125–40.
- Cotterman, C. W. (1940). *A calculus for statistico-genetics*. PhD thesis, The Ohio State University.
- Cowell, R. (2016). Combining allele frequency uncertainty and population substructure corrections in forensic DNA calculations. *Forensic Science International: Genetics*, **23**, 210–6.
- Cowell, R. G., Graversen, T., Lauritzen, S., and Mortera, J. (2015). Analysis of DNA mixtures with artefacts. *Journal of the Royal Statistical Society Series C (with discussion)*, **64**, 1–48.

García, O., Alonso, J., Cano, J., García, R., Luque, G., Martín, P., de Yuso, I. M., Maulini, S., Parra, D., and Yurrebaso, I. (2012). Population genetic data and concordance study for the kits Identifier, NGM, PowerPlex ESX 17 System and Investigator ESSplex in Spain. *Forensic Science International: Genetics*, **6**, (2), e78–9.

Good, I. J. (1979). Studies in the History of Probability and Statistics. XXXVII A. M. Turing's statistical work in World War II. *Biometrika*, **66**, 393–6.

Graversen, T. (2013). *DNAmixtures: Statistical Inference for Mixed Traces of DNA*. R package version 0.1-0, [dnamixtures.r-forge.r-project.org/](https://dnamixtures.r-forge.r-project.org/).

Graversen, T. and Lauritzen, S. (2015). Computational aspects of DNA mixture analysis. *Statistics and Computing*, **25**, 527–41. arXiv:1302.4956.

Green, P. J. (2015). Contribution to Discussion of paper by Cowell, et al. *Journal of the Royal Statistical Society Series C*, **64**, 41.

Green, P. J. (2020a). *KinMix: DNA mixture analysis with related contributors*. R package 2.0, <https://petergreenweb.wordpress.com/kinmix2-0>.

Green, P. J. (2020b). *KinMix User Guide 2.0: DNA mixture analysis with related contributors*. <https://petergreenweb.wordpress.com/kinmix2-0>.

Green, P. J. and Mortera, J. (2009). Sensitivity of inferences in forensic genetics to assumptions about founder genes. *Annals of Applied Statistics*, **3**, 731–63.

Green, P. J. and Mortera, J. (2017). Paternity testing and other inference about relationships from DNA mixtures. *Forensic Science International: Genetics*, **28**, 128–37.

Green, P. J., Mortera, J., and Prieto, L. (2020). Casework applications of probabilistic genotyping methods for DNA mixtures that allow relationships between contributors. Technical report, Universita Roma Tre. In preparation.

Hansson, O. (2017). *persim: Simulation of the Forensic DNA Process*. R package version 1.0.2, <https://CRAN.R-project.org/package=pcrsim>.

Hernandis, E., Dørum, G., and Egeland, T. (2019). relmix: An open source software for DNA mixtures with related contributors. *Forensic Science International: Genetics Supplement Series*, **7**, 221–3.

Jacquard, A. (1974). *The genetic structure of populations*. Springer-Verlag.

Lauritzen, S. L. and Spiegelhalter, D. J. (1988). Local computations with probabilities on graphical structures and their application to expert systems (with discussion). *Journal of the Royal Statistical Society, Series B*, **50**, 157–224.

Mortera, J. (2020). DNA mixtures in forensic investigations: The statistical state of the art. *Annu. Rev. Stat. Appl.*, **7**, 1–34.

Nadot, R. and Vaysseix, G. (1973). Apparentement et identité. Algorithme du calcul des coefficients d'identité. *Biometrics*, **29**, 347–59.

Thompson, E. A. (1974). Gene identities and multiple relationships. *Biometrics*, **30**, 667–80.

Thompson, E. A. (2013). Identity by descent: Variation in meiosis, across genomes, and in populations. *Genetics*, **194**, 301–26.

Tvedebrink, T. (2010). Overdispersion in allelic counts and  $\theta$ -correction in forensic genetics. *Theoretical Population Biology*, **78**, (3), 200 – 210.

Tvedebrink, T., Eriksen, P., and Morling, N. (2015). The multivariate Dirichlet-multinomial distribution and its application in forensic genetics to adjust for subpopulation effects using the  $\theta$ -correction. *Theoretical Population Biology*, **105**, 24–32.

Vigeland, M. D. (2019a). *pedtools: Creating and Working with Pedigrees and Marker Data*. R package version 0.9.0, <https://github.com/magnusdv/pedtools>.

Vigeland, M. D. (2019b). *ribd: Pedigree-based Relatedness Coefficients*. R package version 1.0.0, <https://github.com/magnusdv/ribd>.

Wright, S. (1940). Breeding structure of populations in relation to speciation. *American Naturalist*, **74**, 232–48.

Wright, S. (1951). The genetical structure of populations. *Annals of Eugenics*, **15**, 323–54.

## Supplementary information

### Supplementary section 1: Algorithms in pseudo-code

See Algorithm 1 for the pseudocode for the generative model, that is for generating genotypes from the constructive model of Section 3.2. The algorithm for the construction of the CPTs for the Bayes nets (Sections 3.3 and 3.4) is essentially the same except that random variables are replaced by their probability distributions in table form, as in Algorithm 2.

The notation used is as follows. The input variables are a coding of some of the information illustrated in Table 4:  $\pi$  is one of the permuted patterns that can generate the typed individual genotypes (in this example, 5 in number);  $ncontr$  is the number of mixture contributors whose genotypes's conditional distributions we are modelling (in the example in Table 4, two:  $Fgt$  and  $Mgt$ ), these are numbered  $1 = 1, 2, \dots, ncontr$  in the pseudocode;  $g = 1, 2$  indexes an individual's paternal and maternal genes;  $draw_{\pi ig}$  is a boolean variable, true if the  $g$ th gene of individual  $i$  has to be drawn from the gene pool under permuted pattern  $\pi$ , false if it is determined by the typed genotypes;  $par_{\pi ig}$  is an integer parameter, the allele index if  $draw_{\pi ig}$  is false, a running count of genes to be drawn under this pattern if  $draw_{\pi ig}$  is true;  $p(\pi)$  is the probability distribution of  $\pi$  given the observed genotypes (in this example, given  $Cgt$  and  $GFgt$ );  $ndraws$  is the maximum over  $\pi$  of the number of draws needed under pattern  $\pi$ ;  $(q_a)$  are the allele frequencies and  $q_a^* = q_a / \sum_{b=1}^{a-1} q_b$ . As in our example, so in general, all of these input values are easily determined from the specified IBD pattern distribution and the allele frequencies.

The output variables are the genotype allele count arrays  $(n_{ia})$  for the mixture contributors  $\{i\}$ , whose distribution conditions on the observed typed genotypes of their relatives, together with the latent variables  $\pi$ , the permuted pattern, and  $(m_{ja})$ , the allele count arrays for the founding genes.

---

#### Algorithm 1 The generative model

---

**Input:**  $ndraws, ncontr, (draw_{\pi ig}), (par_{\pi ig}), (q_a), p(\pi)$

**Output:** Sample values from the joint distribution of nodes  $\pi, (m_{ja}), (n_{ia})$

```

1: for  $j \leftarrow 1, 2, \dots, ndraws$  do                                 $\triangleright$  Draws from the gene pool
2:    $m_{j1} \leftarrow Bernoulli(q_1)$ 
3:    $T_{j1} \leftarrow m_{j1}$ 
4:   for  $a \leftarrow 2, 3, \dots, A - 1$  do
5:      $m_{ja} \leftarrow Bernoulli((1 - T_{j,a-1})q_a^*)$ 
6:      $T_{ja} \leftarrow T_{j,a-1} + m_{ja}$ 
7:    $m_{jA} \leftarrow (1 - T_{j,A-1})$ 
8:   Draw  $\pi$  w.p.  $p(\pi)$                                  $\triangleright$  Drawing from pattern distribution
9:   for  $i \leftarrow 1, 2, \dots, ncontr$  do
10:    for  $a \leftarrow 1, 2, \dots, A$  do
11:      for  $g \leftarrow 1, 2$  do
12:        if  $draw_{\pi ig}$  then  $j \leftarrow par_{\pi ig}; h_g \leftarrow m_{ja}$ 
13:        else  $h_g \leftarrow I[par_{\pi ig} = a]$ 
14:       $n_{ia} \leftarrow h_1 + h_2$ 

```

---

---

**Algorithm 2** Constructing CPTs

---

**Input:**  $ndraws, ncontr, (draw_{\pi ig}), (par_{\pi ig}), (q_a), p(\pi)$ 
**Output:** CPTs for a BN with nodes  $\pi, (m_{ja}), (n_{ia})$ 

```

1: for  $j \leftarrow 1, 2, \dots, ndraws$  do                                 $\triangleright$  Draws from the gene pool
2:    $p(m_{j1}) \leftarrow q_1 I[m_{j1} = 1] + (1 - q_1) I[m_{j1} = 0]$ 
3:    $p(T_{j1}) \leftarrow I[T_{j1} = m_{j1}]$ 
4:   for  $a \leftarrow 2, 3, \dots, A - 1$  do
5:      $p(m_{ja} = 1) \leftarrow q_a^* I[T_{j,a-1} = 0] ; p(m_{ja} = 0) = 1 - p(m_{ja} = 1)$ 
6:      $p(T_{ja}) \leftarrow I[T_{ja} = T_{j,a-1} + m_{ja}]$ 
7:    $p(m_{jA}) \leftarrow I[m_{jA} = (1 - T_{j,A-1})]$ 
8: for all  $\pi$  do                                          $\triangleright$  Looping over pattern distribution
9:   for  $i \leftarrow 1, 2, \dots, ncontr$  do
10:    for  $a \leftarrow 1, 2, \dots, A$  do
11:      for  $g \leftarrow 1, 2$  do
12:        if  $draw_{\pi ig}$  then  $j \leftarrow par_{\pi ig}; h_g \leftarrow m_{ja}$ 
13:        else  $h_g \leftarrow I[par_{\pi ig} = a]$ 
14:       $p(n_{ia} | \pi, (m_{ja})) \leftarrow I[n_{ia} = h_1 + h_2]$ 

```

---

## Supplementary section 2: UAF in complex problems involving relationships

Let  $T$  be the typed genotypes,  $C$  the genotypes of the contributors to the mixture,  $M$  the meiosis pattern,  $f$  the founding genes, and  $q$  the allele frequencies.

Then we want  $P(C|T)$ .

Clearly

$$P(C|T) = \frac{P(C, T)}{P(T)} = \frac{\int \sum P(C, T|M, q, f)p(M)p(f|q)p(q)dq}{\int \sum P(T|M, q, f)p(M)p(f|q)p(q)dq}$$

$T$  is a deterministic function of  $M$  and of a subvector of  $f$  we call  $f_{T,M}$ , so the denominator is

$$P(T) = \int \sum P(T|M, q, f)p(M)p(f|q)p(q)dq = \sum_M \sum_{f_{T,M}} P(T|M, f_{T,M})p(M) \int p(f_{T,M}|q)p(q)dq,$$

in which  $P(T|M, f_{T,M})$  is actually an indicator function.

$C$  is a deterministic function of  $M$ ,  $f_{T,M}$  and additional founding genes  $f_{C|T,M}$ , so

$$P(C, T) = \sum_M \sum_{f_{T,M}} \sum_{f_{C|T,M}} P(C|M, f_{T,M}, f_{C|T,M})P(T|M, f_{T,M})p(M) \int p(f_{T,M}|q)p(f_{C|T,M}|q)p(q)dq$$

### Dirichlet–Multinomial

$p(f_{T,M}|q)$  and  $p(f_{C|T,M}|q)$  are polynomials in  $q$ , and  $p(q)$  is a Dirichlet distribution, so  $\int p(f_{T,M}|q)p(q)dq$  and  $\int p(f_{T,M}|q)p(f_{C|T,M}|q)p(q)dq$  are explicit (expressed in terms of Gamma functions).

Suppose that the allele frequencies  $q$  have a Dirichlet prior:  $p(q) = \prod_a q_a^{\delta_a - 1} \times \Gamma(\sum_a \delta_a) / \prod_a \Gamma(\delta_a)$ , and that  $f_{T,M}$  consists of  $n_a$  copies of allele  $a$ ,  $a = 1, 2, \dots, A$ . Then  $p(f_{T,M}) = \prod_a q_a^{n_a}$  and

$$\int p(f_{T,M})p(q)dq = \int \prod_a q_a^{\delta_a + n_a - 1} dq \times \frac{\Gamma(\sum_a \delta_a)}{\prod_a \Gamma(\delta_a)} = \frac{\Gamma(\sum_a \delta_a) \prod_a \Gamma(\delta_a + n_a)}{\Gamma(\sum_a (\delta_a + n_a)) \prod_a \Gamma(\delta_a)} = DM(n; \delta),$$

say. Similarly, if  $f_{C|T,M}$  has  $n'_a$  copies of allele a, then

$$\int p(f_{T,M}|q)p(f_{C|T,M}|q)p(q)dq = \frac{\Gamma(\sum_a \delta_a) \prod_a \Gamma(\delta_a + n_a + n'_a)}{\Gamma(\sum_a (\delta_a + n_a + n'_a)) \prod_a \Gamma(\delta_a)} = DM(n + n'; \delta).$$

(These Dirichlet–Multinomial distributions are what is evaluated in the Pólya urn BN.)

### Computation of $P(C|T)$

$T$  is observed, so we only need  $P(T|M, f_{T,M})$  for a single value of  $T$ , and therefore  $P(T)$  becomes an explicit sum over  $M$  and  $f_{T,M}$ , with only a small number of non-zero terms.

We need  $P(C|T)$  for all possible values of  $C$ , so to compute  $P(C|T)$  we use a BN whose nodes include  $f_{C|T,M}$  and  $M$  ( $T$  being now fixed and  $f_{T,M}$  a fixed function of  $M$ ). In this BN, if the evidence and joint probability has product  $P(C, T)/P(T)$ , then the normalising constant will evaluate  $P(C|T)$ .

$$\begin{aligned} P(C, T)/P(T) &= \\ &= P(T)^{-1} \sum_M \sum_{f_{T,M}} \sum_{f_{C|T,M}} P(C|M, f_{T,M}, f_{C|T,M}) P(T|M, f_{T,M}) p(M) DM(n + n'; \delta) \\ &= P(T)^{-1} \sum_M \sum_{f_{T,M}} \sum_{f_{C|T,M}} P(C|M, f_{T,M}, f_{C|T,M}) P(T|M, f_{T,M}) p(M) DM(n'; n + \delta) DM(n; \delta) \end{aligned}$$

Of the terms in this expression,  $P(T)$ ,  $\{\delta_a\}$ ,  $\{n_a\}$  are constants,  $P(C|M, f_{T,M}, f_{C|T,M})$  and  $P(T|M, f_{T,M})$  are indicator functions. Write  $p^*(M) = P(T)^{-1} p(M) \sum_{f_{T,M}} P(T|M, f_{T,M}) DM(n; \delta)$  (which is explicitly available but may not be correctly normalised), then

$$P(C, T)/P(T) = \sum_M \sum_{f_{C|T,M}} P(C|M, f_{T,M}, f_{C|T,M}) p^*(M) DM(n'; n + \delta).$$

However, note that  $n$  are the allele counts corresponding to  $f_{T,M}$ , so for fixed  $T$  vary with  $M$ . This means that the Pólya urn component of the BN will have the node corresponding to  $M$  as an additional parent. Alternatively, we have to loop over  $M$ , running a separate BN for each value (for which  $p^*(M)$  is non-zero), and combining them afterwards.